National Technical University of Athens (N.T.U.A.)
School of Chemical Engineering
Department of Process Analysis and Plant Design

Numerical Solution of Population Balance Equations with the Maximum Entropy Method of Moments.

Master of Science in Computational Mechanics
Diploma Thesis

by,
Athanasios Zisimos

Supervisor:

Assistant Professor Michail Kavousanakis

Athens, June 2021

Intentionally left blank page

Εθνικό Μετσόβιο Πολυτεχνείο (Ε.Μ.Π.)
Σχολή Χημικών Μηχανικών
Τομέας Ανάλυσης, Σχεδιασμού και Ανάπτυξης Διεργασιών και Συστημάτων

Αριθμητική Επίλυση Ισοζυγίων Κυτταρικών Πληθυσμών με τη Μέθοδο των Ροπών και της Μέγιστης Εντροπίας.

Μεταπτυχιακό Δίπλωμα Ειδίκευσης στην Υπολογιστική Μηχανική
Διπλωματική Εργασία

του,
Αθανάσιου Ζήσιμου

Επιβλέπων Καθηγητής:

Επίκουρος Καθηγητής Μιχαήλ Καβουσανάκης

Αθήνα, Ιούνιος 2021

Intentionally left blank page

National Technical University of Athens (N.T.U.A.)
School of Chemical Engineering
Department of Process Analysis and Plant Design

Numerical Solution of Population Balance Equations with the Maximum Entropy Method of Moments.

by,
Athanasios Zisimos

Supervisor:
Assistant Professor Michail Kavousanakis

Athens, June 2021

Intentionally left blank page

Εθνικό Μετσόβιο Πολυτεχνείο (Ε.Μ.Π.)
Σχολή Χημικών Μηχανικών
Τομέας Ανάλυσης, Σχεδιασμού και Ανάπτυξης Διεργασιών και Συστημάτων

Αριθμητική Επίλυση Ισοζυγίων Κυτταρικών Πληθυσμών με τη Μέθοδο των Ροπών και της Μέγιστης Εντροπίας.

του,
Αθανάσιου Ζήσιμου

Επιβλέπων Καθηγητής:
Επίκουρος Καθηγητής Μιχαήλ Καβουσανάκης

Αθήνα, Ιούνιος 2021

Intentionally left blank page

Dedicated to my parents
Evangelos and Panorea,
and my brother George
for their unconditional
love and support.

Intentionally left blank page

Abstract

There is a plethora of evidence that cell populations are heterogeneous systems in the sense that properties such as size, shape, DNA and RNA content are unevenly distributed amongst the cells of the population. The quantitative understanding of heterogeneity is of great significance, since neglecting its effect can lead to false predictions. Cell population balance models are used to address the implications of heterogeneity and can accurately capture the dynamics of heterogeneous cell population. In particular, cell population balance equations are first-order partial-integro-differential equations and due to the complexity of formulation, analytical solutions are hard to obtain in the majority of cases. Despite the recent progress, the efficient solution of cell population balance models remains a challenging task **(Kavousanakis et al. 2009)**.

At first the modeling of cellular heterogeneity in Lac Operon, a model which is solved using a free boundary algorithm **(Kavousanakis et al. 2009)** was analyzed thoroughly. Furthermore the importance of studying the cells as individuals was presented and the way of treating the cells as individuals and not as homogeneous sets, neglecting their heterogeneity was developed.

Next to that, the cell population balance equations were analytically presented and each term of the Lac Operon model was studied one by one. All the components of the model such as birth rate, death rate, the partition probability density function, the boundary conditions and formulas were presented. Numerical methods, including the finite differences method, the finite elements method and spectral methods that are usually employed for the solution of most population balance equations were referred, but basically an alternative to these methods, the so called method of moments as a tool for the solution of the cell population balance equations was described **(Randolph and Larson 1971)**.

In addition, the maximum entropy method as a tool for the solution of partial-integro-differential systems of equations was studied carefully. The way maximum entropy method works in order to reconstruct the density function given a known set of moments was presented thoroughly. Furthermore, it was analyzed the way that one given a number of known moments for a given observation, is able to find a unique distribution responsible for generating those moments **(Abboud et al. 2015).** Additionally, the fact that the maximum entropy method is based on the concept that the distribution that maximizes the information entropy is the one that is statistically most likely to occur was persistently analyzed **(Mead and Papanicolaou 1984)**.

In the last part of this diploma thesis, a comparison between the maximum entropy method of moments and the numerical solution of the CPB problem with the finite elements method was presented. The convergence between the two solutions was observed for different number of moments. Furthermore, suggestions for future work like the solution of the CPB problem in two or higher dimensions and the possibility of implementing steady-state algorithms (Newton-Raphson), parametric continuation algorithms (pseudo arc-length continuation), and eigenvalue solvers wrapped around the maximum entropy method of moments were given.

Περίληψη

Υπάρχει πληθώρα ερευνητικών αποτελεσμάτων ότι τα ισοζύγια κυτταρικών πληθυσμών είναι ανομοιογενή συστήματα, υπό την έννοια ότι το μέγεθος, το σχήμα και το ενδοκυτταρικό περιεχόμενο σε DNA και RNA είναι ανισομερώς κατανεμημένο μεταξύ των κυττάρων του κυτταρικού πληθυσμού. Η εις βάθος κατανόηση της ετερογένειας είναι πολύ σημαντική, διότι η αγνόηση αυτής μπορεί να οδηγήσει σε εσφαλμένες προβλέψεις. Τα ισοζύγια κυτταρικών πληθυσμών χρησιμοποιούνται για να διατυπώσουν τις επιπτώσεις της ετερογένειας των κυτταρικών πληθυσμών και να βοηθήσουν στην σύλληψη της δυναμικής απόκρισης της ετερογένειας αυτών. Πιο συγκεκριμένα, τα ισοζύγια κυτταρικών πληθυσμών αποτελούν πρωτοβάθμιες μερικές διαφορικές εξισώσεις και λόγω της περιπλοκότητας της διατύπωσής τους, τις περισσότερες φορές είναι δύσκολο να επιλυθούν αναλυτικά. Παρά τις τελευταίες εξελίξεις, η επίλυσή τους παραμένει ένα απαιτητικό εγχείρημα **(Kavousanakis et al. 2009)**.

Αρχικά, η μοντελοποίηση της κυτταρικής ετερογένειας του Lac Operon, ενός μοντέλου το οποίο επιλύεται χρησιμοποιώντας έναν αλγόριθμο ελεύθερου συνόρου **(Kavousanakis et al. 2009)**, αναλύθηκε διεξοδικά. Επιπροσθέτως, παρουσιάστηκε η κρισιμότητα της ανάλυσης των κυττάρων ως μονάδες και αναλύθηκε ο τρόπος να διαχειρίζεται κανείς τα κύτταρα ατομικά και όχι ως ομογενή σύνολα, αγνοώντας την επίδραση της ετερογένειας.

Εν συνεχεία, οι εξισώσεις των ισοζυγίων των κυτταρικών πληθυσμών παρουσιάστηκαν αναλυτικά και μελετήθηκε και επεξηγήθηκε κάθε όρος του Lac Operon πολύ προσεκτικά. Όλοι οι παράγοντες του μοντέλου, όπως ο ρυθμός γέννησης, ο ρυθμός θανάτωσης, η συνάρτηση πυκνότητας πιθανότητας, οι συνοριακές συνθήκες και όλες οι εξισώσεις, παρουσιάστηκαν διεξοδικώς. Επίσης, έγινε αναφορά σε αριθμητικές μεθόδους, οι οποίες αξιοποιούνται για την επίλυση ισοζυγίων κυτταρικών πληθυσμών, όπως η μέθοδος των πεπερασμένων διαφορών, η μέθοδος των πεπερασμένων στοιχείων, φασματικές μέθοδοι, αλλά κυρίως παρουσιάστηκε η μέθοδος της μέγιστης εντροπίας, η οποία αξιοποιήθηκε ως εργαλείο για την επίλυση των ισοζυγίων κυτταρικών πληθυσμών **(Randolph and Larson 1971)**.

Επίσης, μελετήθηκε η μέθοδος της μέγιστης εντροπίας ως εργαλείο για την επίλυση συστημάτων μερικών διαφορικών εξισώσεων. Παρουσιάστηκε ο τρόπος με τον οποίο γίνεται η ανακατασκευή της συνάρτησης πυκνότητας, δοθέντος ενός αριθμού ροπών. Ακόμη, αναλύθηκε ο τρόπος με τον οποίο κάποιος που του έχει δοθεί ένας συγκεκριμένος αριθμός ροπών μπορεί να καταλήξει σε μια μοναδική συνάρτηση πυκνότητας η οποία προκύπτει από τις εν λόγω ροπές **(Abboud et al. 2015)** και παρουσιάστηκε η μέθοδος της μέγιστης εντροπίας, η οποία βασίζεται στο γεγονός, πως η κατανομή η οποία μεγιστοποιεί την εντροπία είναι αυτή η οποία είναι πιο πιθανό να συμβεί **(Mead and Papanicolaou 1984)**.

Στο τελευταίο μέρος αυτής της διπλωματικής εργασίας, παρουσιάστηκε η σύγκριση μεταξύ των αποτελεσμάτων τα οποία προέκυψαν από την επίλυση των ισοζυγίων κυτταρικών πληθυσμών με τη μέθοδο της μέγιστης εντροπίας των ροπών και με τη μέθοδο των πεπερασμένων στοιχείων. Η σύγκριση μεταξύ των αποτελεσμάτων των δύο μεθόδων παρατηρήθηκε για διάφορους αριθμούς ροπών. Επίσης, δόθηκαν και

προτάσεις για μελλοντική έρευνα, ως προς την επίλυση ισοζυγίων κυτταρικών πληθυσμών στις δύο ή στις τρεις διαστάσεις, καθώς και η πιθανότητα επίλυσής τους μέσω της εφαρμογής αλγορίθμων, όπως είναι η μέθοδος Newton-Raphson, η μέθοδος pseudo arc-length continuation, αλλά και με επιλύτες ιδιοτιμών, όλοι βασισμένοι στη μέθοδο της μέγιστης εντροπίας των ροπών.

Acknowledgements

*To my **family**, for their sincere love and support, for always being there for me and supporting my choices. For teaching me the beauty of music, books and science and advising me to love the simple things and be grateful to God and people, because people are people and we are allowed to make mistakes…*

*To **professor Kavousanakis** or I should better say our **Mihalis**, for believing in me and allowing me to be a part of his research and consequently his life. For not being just a professor, but mainly a teacher. For being kind, generous, curious, passionate and supportive. For pushing me always to go a step further and find the solution of the problem. For always being there for me during this beautiful journey….*

*To **National Technical University of Athens**, for accepting me and giving me the chance to get a step closer to my dreams and for teaching me that an engineer must never losing his faith in science and people, because there will always be people who will believe too…*

*To **life**, that has taught me that when a man fights for the things he wants, at the end of the day he is going to make it happen, because everything is untouchable until you put it in your head. After that it is in your hand to turn dream into reality…*

Contents

Intentionally left blank page

1 Modeling of cellular heterogeneity in Lac Operon

Recent developments in molecular biology provide us with a lot of interesting and significant tools for the study of biochemical processes, not only at the single-cell level but also at the cell population level. There is a plethora of systemic biology techniques, which have been used, in order to understand complex cellular processes. However, the phenotypic behavior of a cellular population is not solely the result of the interactions between the numerous ingredients in each of the individual cells, but also arises as the result of the complexity, the direct and indirect interactions between the cells of a cellular population and their microenvironment. The intercellular and intracellular interactions lead to important phenotypic fluctuations from one cell to another and this biological phenomenon is known as heterogeneity. These phenomena have been observed in numerous biological systems, e.g. in systems which contain merges of genes and lacZ **(Aviziotis et al. 2015)**.

The main goal of most of the medical applications and approaches, which consider pathological conditions, is the handling of the cell population as a whole and not the handling of each cell individually. All of the experimental techniques, which are available to engineers such as DNA sequences, liquid chromatography, mass phasmatometry, use digital information and data, which correspond to a cell population and not to cell individuals. The heterogeneity of cell population can lead to inhibition of efficient production biotechnology products and their reduced ability to adapt to abrupt environmental changes. Therefore, understanding the dynamic relationship between the phenomena that take place at both the cell individual level and the cell population level could provide with significant insight and information on the detection, prognosis and treatment of various diseases, such as cancer **(Mantzaris 2006)**. As a consequence, the dynamic evolution of all the phenomena which take place should be studied in depth, because the right mathematical approach to solution of the problem is a means to better understand the various sub-processes and the effect of heterogeneity on the population phenotype.

A lot of researchers have made the assumption that cell individuals act in a homogeneous manner, but in reality cell individuals act differently during a specific time period. For example, if one examines resistance and death rates in a cellular population, it is the older cells that are more resistant and their death rate is smaller. On the other hand, young cells tend to protect older cells, as a result young cells die trying to protect the older one. Consequently, the older cells present a small death rate and remain untouchable, but this is actually something undesired **(Mantzaris 2007)**.

The heterogeneity in isogenic cell populations where each cell carries the same genetic network originates from two basic independent sources. The first source of heterogeneity comes from the unequal distribution of the amounts of the majority of intracellular components of mother cells (with the exception of DNA) between the daughter cells and this phenomenon is known as extrinsic heterogeneity. When mitosis occurs the content is unevenly distributed amongst the daughter cells. This phenomenon is repeated after each cell cycle and further enhances heterogeneity. This exact variation of the intracellular content of the daughter cells leads to different phenotypes. **(Elowitz et al. 2002)** proved that this type of heterogeneity has been the most significant one for a wide range of induction levels in various E. coli strains.

The second source of heterogeneity is called intrinsic heterogeneity. Regulatory molecules which control the cellular phenotype are found in very low concentrations. Furthermore, regulatory molecules control the rate of intracellular reactions, and this is the reason one can observe random fluctuations in their rates leading even to different cellular phenotypic behavior. **(Mantzaris 2007)**.

The basic target of the population balance modeling approach is to investigate how the phenotypic variance at the single-cell level is inherited to the population. The heterogeneity of the cell population, which affects the behavior of the entire cell population, demands to study the whole phenomenon as a dynamic procedure. The mathematical models developed can: (a) take into consideration the intrinsic heterogeneity amongst the cells of the isogenic population and (b) include the mathematical formulation of the intracellular processes characterizing the gene regulatory network at each cell **(Kavousanakis et al. 2009)**.

In CPB models the unknown variable is the number of cells, which at time t have intracellular content between x and x+dx. CPBs are non linear partial-integro-differential equations and in general can be solved using numerical and not analytical methods. During the years population balance equations were solved by a number of numerical methods, such as the method of weighted residuals using global shape functions **(Subramanian and Ramkrishna 1971)**, the method of finite elements using orthogonal collocation **(Zhu et al. 2000)** and spectral methods **(Mantzaris et al. 2001)**.

For CPB problems with *a priori* unknown boundaries of the physiological state space, free boundary algorithms have been developed **(Kavousanakis et al. 2009)**. In this work, they illustrated the efficiency of the algorithm for the isogenic populations carrying plasmids of positive feedback architectures, and the genetic network of interest was Lac Operon. This genetic network illustrates a non linear behavior, resulting in bistable behavior over a significant region of extracellular inducer concentrations. CPBs were utilized in order to answer the question whether the bistable behavior observed at the single cell level is also present at the population level.

However, numerical methods solving for the density function of cells can have significant computational requirements. An alternative to these approaches is the solution of the CPB problem utilizing the method of moments. The original CPB problem is expressed in terms of the number density function's statistical moments, and we study the evolution of the moments (rather than the density function). In the general case, formulating the equations as a function of moments requires a closure for the density function. In this thesis we utilize the maximum entropy method; in particular, at each time instance we reconstruct the density function given a small number of moments (problem of moments) based on the maximum entropy methodology. In particular, given a number of moments we construct a distribution p(x) that maximizes Shanon's entropy, S. The method of moments using the maximum entropy is presented and compared against the finite elements method, which solves for the density function.

2 Mathematical modeling of cellular heterogeneity: cell population balance models

2.1 Cell population balance models for isogenic cells

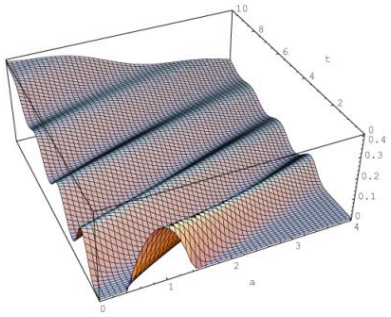

Figure 2.1. Solution of linear age structured cell population balance model.

CPBs for isogenic cells are developed in a way so that they can incorporate the dynamics of intracellular reactions (i.e., incorporate the dynamics of the genetic network) and simultaneously model the dynamics of a cell population taking into account the growth, death and mitosis dynamics of each cell.

CPBs (Cell Population Balance Models) are partial-integro-differential equations, with unknown variable the cells per volume unit $F(\mathrm{x},\mathrm{t})\,\mathrm{dx}$ that for a specific time t has intracellular content between x and x+dx. The dynamics of the distribution function $\boldsymbol{F}(\mathrm{x},\mathrm{t})$ is given by the following deterministic model (ignoring the stochastic processes modeling intrinsic heterogeneity):

$$\frac{\partial F(\mathrm{x},\mathrm{t})}{\partial t}+\frac{\partial\left[R(x)F(x,t)\right]}{\partial x}+\Gamma(x)F(x,t)=\ldots$$
$$2\int_{x}^{x_{\max}}\Gamma(x')P(x,x')F(x',t)\,\mathrm{dx}' \qquad (2.1)$$

$\frac{\partial \boldsymbol{F}(\mathrm{x},\mathrm{t})}{\partial \boldsymbol{t}}:$	time derivative of distribution function,
$\frac{\partial\left[\boldsymbol{R}(\boldsymbol{x})\boldsymbol{F}(\boldsymbol{x},\boldsymbol{t})\right]}{\partial \boldsymbol{x}}:$	increase rate, which takes into account the cell loss due to the volume increase,
$\Gamma(\boldsymbol{x})\boldsymbol{F}(\boldsymbol{x},\boldsymbol{t}):$	transfer term, due to cell loss during their transfer to the next phase,
$2\int_{x}^{x_{\max}}\Gamma(\boldsymbol{x}')\boldsymbol{P}(\boldsymbol{x},\boldsymbol{x}')\boldsymbol{F}(\boldsymbol{x}',\boldsymbol{t})\,\mathrm{dx}':$	birth rate, which describes birth of cells of intracellular content x from the division of all cells with greater intracellular content. The integral is multiplied by two, because during birth each cell divides into 2 cells.
$\boldsymbol{P}(\boldsymbol{x},\boldsymbol{x}'):$	Partition distribution function, which describes the fraction of intracellular content which is transferred to each of the daughter cells during division,

An alternative formulation of the deterministic model above is given by the following formula which takes into consideration the probability density function, which describes the number of cells with intracellular content x during time t divided by the total number of cells at the same time.

$$\frac{\partial n(\mathrm{x},\mathrm{t})}{\partial t}+\frac{\partial\left[R(x)n(x,t)\right]}{\partial x}+\Gamma(x)n(x,t)=\ldots$$
$$2\int_{x}^{x_{\max}}\Gamma(x')P(x,x')n(x',t)\,\mathrm{dx}'-n(x,t)\int_{0}^{x_{\max}}\Gamma(x)n(x,t)\,\mathrm{dx} \qquad (2.2)$$

$\frac{\partial \boldsymbol{n}(\mathrm{x},\mathrm{t})}{\partial \boldsymbol{t}}:$	Accumulation of cells with intracellular content x in the control volume.
$\frac{\partial\left[\boldsymbol{R}(\boldsymbol{x})\boldsymbol{n}(\boldsymbol{x},\boldsymbol{t})\right]}{\partial \boldsymbol{x}}:$	Loss rate, by which cells with intracellular content x get lost from this content due to intracellular reactions.
$\Gamma(\boldsymbol{x})\boldsymbol{n}(\boldsymbol{x},\boldsymbol{t}):$	Rate at which cells with intracellular content x are "consumed" due to cellular mitosis, which leads to the creation of cells with intracellular content which is less than x.
$2\int_{\boldsymbol{x}}^{\boldsymbol{x}_{\max}}\Gamma(\boldsymbol{x}')\boldsymbol{P}(\boldsymbol{x},\boldsymbol{x}')\boldsymbol{n}(\boldsymbol{x}',\boldsymbol{t})\,\mathrm{dx}':$	Birth rate, which describes birth of cells of intracellular content x from the division of all cells with greater intracellular content.
$\boldsymbol{n}(\boldsymbol{x},\boldsymbol{t})\int_{0}^{\boldsymbol{x}_{\max}}\Gamma(\boldsymbol{x})\boldsymbol{n}(\boldsymbol{x},\boldsymbol{t})\,\mathrm{dx}:$	Dilution term, which is derived from (2.1) when expressed in terms of n(x,t). This term makes sure that we end up in a steady state solution (because cells at a space interval x, x+dx are divided by the total number of cells).

In order to obtain a unique solution for the (2.2) we need to impose appropriate boundary conditions. Here, we apply the following containment boundary conditions.

$$n(0,t)=n(\mathrm{x}_{\max},t)=0 \qquad (2.3)$$

The unknown function in (2.2) is the function $n(\mathrm{x},t)$, which is the probability density function (PDF). Probability density function has to satisfy condition (2.4),

$$\int_{0}^{x_{\max}}n(\mathrm{x},t)dx=1 \qquad (2.4)$$

According to Equation 2.2 the dynamic behavior of a cell population is defined completely by 3 functions, which are widely known in the bibliography as Intrinsic Physiological State Functions (IPSF) and they formulate processes that occur at the single-cell level.

2.2 Intrinsic physiological state functions (IPSF)

$\boldsymbol{R}(x):$	Network of chemical reactions, which contains rates of production of all intracellular species described in the model.
$\Gamma(\boldsymbol{x}):$	Single-cell division rate, which describes the rate at which a cell with content x is divided into two daughter cells.
$\boldsymbol{P}(\boldsymbol{x},\boldsymbol{x}'):$	Partition density function, which describes the probability by which a mother cell with intracellular content x', gives birth to a daughter cell of content x and a daughter cell of content x'-x.

2.3 Genetic network with positive feedback architecture

The genetic network which is being under investigation is called Lac Operon (Figure 2.2). It is comprised of the promoter lac P, from the operator lac O and three genes that encode the proteins which are important for the metabolism of lactose. Lac Y encodes lac permease, which contributes to the transportation of lactose or something analogue to her, like IPTG (Isopropyl β-D-1-Thiogalactopyranoside) inside the cell. Furthermore, lac Z encodes enzyme β-galactosidase and lac A (transacetylase) **(Kavousanakis et al. 2009)**.

The inhibitor lac I binds to the operator site (part of DNA prior of the three genes of Lac Operon) and prevents binding of the RNA polymerase, thus inhibiting transcription of the genes' DNA into the corresponding mRNA.

However, in the presence of lactose, TMG or IPTG, the inducer is transported into the cell (via diffusion initially), where it binds to the lac I repressor in a bimolecular reaction. Thus, some operator becomes free of lac I and the transcription is initiated. Upon expression of lac Y, further transport of the inducer occurs at a higher rate and as a result, further expression of the three Lac Operon genes is initiated. Thus, in this network, the expression of lac Y gene enhances further expression of itself and in this sense the network functions as an autocatalytic system or a positive feedback loop. It is well known that such networks exhibit bistable behavior at the single-cell level **(Mantzaris 2007)**. The arising question is whether this property is inherited to the cell population level. The answer to this question can be given initially by formulating a simple mathematical model, which captures the basic features of the positive feedback loop architecture **(Mantzaris 2005)**.

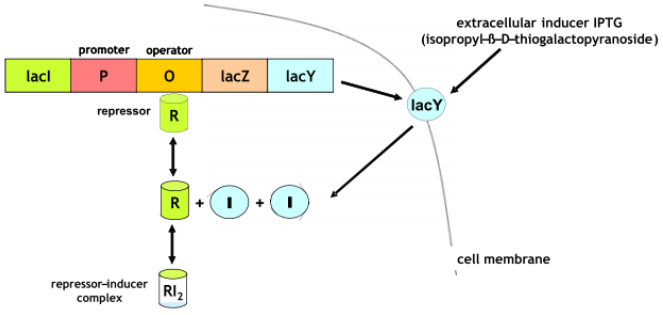

Figure 2.2. Schematic of the positive feedback loop network, Lac Operon with IPTG induction.

A simplified network of the intracellular reactions is provided by the following reaction set **(Kepler and Elston 2001)**.

$O_0 \xrightarrow{k_0} Y$ $O_1 \xrightarrow{k_1} Y$ $Y \xrightarrow{\lambda} \varnothing$ $O_0 + Z \underset{\alpha\varphi}{\overset{\varphi}{\rightleftarrows}} O_1$ $Y + Y \underset{\beta x}{\overset{x}{\rightleftarrows}} Z$	2.3

***O*₀, *O*₁**: Fraction of free and occupied operator sites,

Y: monomer produced by the gene expression in either the occupied or the unoccupied state of the operator,

***k*₀, *k*₁**: rate constant of gene expression in the unoccupied state and in the occupied state respectively,

Z: dimer of the gene product, which binds to a free operator resulting an occupied site,

λ: degradation rate constant

Under the assumption that the production rates of monomer product are proportional to the fractions of unoccupied and occupied sites and that the degradation of Y is a first-order reaction, the single-cell monomer dynamics are described by,

$\frac{dY}{dt} = k_0 O_0 + k_1 O_1 - \lambda Y$	2.4
$O_0 + O_1 = 1$	2.5
$O_0 Z = a O_1$	2.6
$Y^2 = \beta Z$	2.7

The basic assumption of the whole procedure is that occupied and unoccupied states are in equilibrium with each other and the same happens for the division mechanism. With the substitution of Equations 2.7 - 2.9 into Equation 2.6 yields,

$\frac{dY}{d\tau} = \frac{k_0 \alpha\beta + k_1 Y^2}{\alpha\beta + Y^2} - \lambda Y$	2.8

By non dimensionalizating the intracellular content Y and time t, we can reduce the number of the parameters in Equation 2.10 as,

$x = \frac{Y}{Y^*}$	2.9
$t = \frac{\tau}{\tau^*}$	2.10

Setting:

$\frac{k_1 t^*}{Y^*} = 1$	2.11
$\pi = \frac{k_0}{k_1}$	2.12
$p = \frac{\alpha\beta}{Y^2_1}$	2.13
$\delta = \lambda t^*$	2.14

and substituting into (2.11 - 2.16) yields the following dimensionless production rate of the dimensionless lac Y amount (the intracellular content x) **(Kavousanakis et al. 2009)**:

$\frac{dx}{dt} = R(x) = \frac{\pi p + x^2}{p + x^2} - \delta x$	2.15

In this model the rate of x change consists of a nonlinear production term and a degradation term. The three dimensionless parameters that are observed are as follows,

π : relative rate of expression when the operator is free and occupied. The rate of gene expression in the unoccupied state is significantly lower than that in the occupied state, which suggests that $\pi << 1$ **(Mantzaris 2007)**,

p : inversely proportional to the extracellular inducer concentration,

δ : dimensionless degradation rate of gene lac Y.

For the scientific solidarity and consistency of the model, the division rate as a function of the intracellular content ($\Gamma(\boldsymbol{x})$) and the partition function ($\boldsymbol{P}(\boldsymbol{x}, \boldsymbol{x}')$) which describes the distribution of the intracellular content during the cellular division to the two newborn daughter cells, are defined and analyzed as follows. The division rate is given from:

$\Gamma(x) = \left(\frac{x}{\langle x \rangle} \right)^L$	2.16

This way of expression of the division of the intracellular content has been applied in a plethora of theoretical and computational approaches of the problem of CPBs **(Mantzaris 2007)**. The basic purpose for a choice like that is that this expression describes experimental data of cell population yeast. A formula for the partition distribution function is:

$$P(x,x') = \frac{1}{2f}\delta(fx' - x) + \frac{1}{2(1-f)}\delta((1-f)x' - x) \qquad (2.17)$$

where δ is the Dirac function and f is the fraction of intracellular content which is given by the mother cell to the smaller daughter cell. It is obvious from this definition that f ranges from 0 to 0.5. In case that $f = 0.5$, symmetric division events are observed, on the other hand, low values of f correspond to more asymmetric division events during the cellular division.

The above formulation corresponds to the case of discrete partitioning. However, there is also an alternative formulation, which is called symmetric partitioning. In this case the partition density function is a continuous function. More precisely, watching the following equation one can observe that the given from the mother cells to the daughter cells intracellular content is no longer a constant fraction of the content. The reason is that the intracellular content is given by the mother cells to the daughter cells with a specific probability.

$$P(x,y) = \frac{1}{y}\frac{\Gamma amma(2q+2)}{\Gamma amma(q+1)\Gamma amma(q+1)}\left(\frac{x}{y}\right)^q\left(1-\frac{x}{y}\right)^q \xrightarrow{\psi = \frac{y}{x_{\max}}} \ldots$$

$$P(\xi,\psi) = \frac{1}{x_{\max}}\frac{1}{\psi}\frac{\Gamma amma(2q+2)}{\Gamma amma(q+1)\Gamma amma(q+1)}\left(\frac{\xi}{\psi}\right)^q\left(1-\frac{\xi}{\psi}\right)^q \qquad (2.18)$$

q: the continuous and symmetric partitioning,

Γamma: is a function defined for real x>0 by the integral $\Gamma amma(x) = \int_0^\infty e^{-t}t^{x-1}dt$

The mathematical model which was described above is an approach of the problem of CPBs, which though does not take into consideration the “randomness” that characterizes small cell populations. Although there are a lot of methods, which are appropriate to study the randomness of a problem like that (Monte Carlo, Karhunen Loeve, etc), in the current Diploma Thesis we solve the model above using the maximum entropy method of moments. Additionally it must be pointed the fact that the computation of the solution of a CPB problem is difficult and time consuming. CPB models are a system of partial-integro-differential equations, which needs special treatment and increases the computational requirements. We present an alternative approach based on the method of the maximum entropy method of moments, which saves us time, reduces computational cost and helps us end up faster to a solution.

3 Numerical solution of cell population balance models with the maximum entropy method of moments

3.1 From the method of moments to the maximum entropy method

Population balance equations (PBE) are widely used as modeling tool for particulate systems that estimate the dynamic evolution of particle size distribution (PSD) as a function of process operating conditions. They have been used in crystallization, granulation and milling to support process design, optimization and control. Analytical solutions of PBE are available for only special cases. Therefore, numerical methods are usually employed for their solution. These numerical methods can be broadly classified into two main categories: the class of the methods that solve directly for the number density (e.g. least square method, Monte Carlo methods **(Lin et al. 2002),** the discrete population balance methods (DPB) methods **(Hounslow et al. 1988)** and the class of methods that solve for the moments of the number density **(Diemer and Olson 2002)**. The most applicable methods for the solution of the population balance models are the DPB methods. The greatest advantage of DPB methods is that they calculate the distribution directly, whereas the main disadvantages are the computational resources required **(Ramkrishna 2008)**.

An alternative to the DPB is the method of moments (MEM). The method of moments involve the conversion of the PBE to equations in terms of the moments of the number density. MOMs therefore have better computational efficiency compared to the DPB and other approaches, and are particularly used for process flowsheet simulations and coupling with fluid flows. The MOM solve for the moments in place of distribution and in some cases moments are all that are required for comparison with experimental data. The standard method of moments is limited to specific growth rate expression, breakage and aggregation kernels **(Falola et al. 2013)**. The basic reason is that for growth rate expression, breakage and aggregation kernels, the moments equations are not closed. The basic question arisen is, how can someone pick a closure for the moment equations. There are three ways of providing closures for the moments equations: (1) Under the assumption that the functional form of the size distribution is known a priori **(Lee 1983)**. (2) Moments interpolation or assumption of dependence of moments **(Frenklach 2002)**. (3) Moments inversion **(Diemer and Olson 2002)**.

Among the three approaches the third one is the most popular; one particular method is the Quadrature Method of Moments (QMOM). The basic disadvantage of QMOMS is that one loses the density function, which is approximated as a collection of Dirac pulses (a representation which is far from reality). However QMOM has been applied in various fluid flow simulations of particulate processes, and it was first developed by **(McGraw 1997).** In this thesis we apply an alternative technique for the reconstruction of the density function, given a small set of low order moments, and this technique is the maximum entropy method, which produces smoother density functions, compared to the ones QMOM generates.

3.2 Maximum entropy method

The maximum entropy method is based on the concept that the distribution that maximizes the information entropy is the one that is statistically most likely to occur. The average rate at which information is produced by a system is called information entropy. Furthermore entropy can be defined as a measure for how much of a system is unknown. Higher information entropy means one knows less about a process. The system with maximum information entropy is the most probable to exist because it is the system in which the least amount of information has been defined. The mathematical formulation of the information entropy S, of a distribution $\eta(x)$, is given by the integral, where Ω is the support of the distribution **(Mead and Papanicolaou 1984)**,

$$S = -\int_{\Omega} \eta(x) \ln \eta(x) dx, \tag{3.1}$$

Given a known number of moments for $\eta(x)$, one has to find the distribution $\eta(x)$ which maximizes S subject to those known moments. Our basic purpose is to calculate the distribution $\eta(x)$ which maximizes the information entropy S subject to the following equation,

$$\int_{\Omega} x^k \eta(x) dx = \mu_k; \; k = 0,1,... \tag{3.2}$$

λ_k: $N+1$ is the number of the unknown moments

μ_k: given finite number of moments for $0 \le k \le N$.

By introducing Lagrangian multipliers one can define the entropy functional as follows,

$$H = \int_{\Omega} \left[-\eta(x) \ln \eta(x) + \sum_{k=0}^{N} \lambda_k x^k \eta(x) \right] dx - \sum_{k=0}^{N} \lambda_k \mu_k \tag{3.3}$$

This functional reaches a maximum when the functional derivatives of H with respect to $\eta(x)$ and λ_k are zero: $\frac{\delta H}{\delta \lambda_k} = 0$ and $\frac{\delta H}{\delta n(x)} = 0$. The first of these derivatives does not provide us with any additional information since it returns the constraints defined in (3.2). However, the second of these derivatives, evaluates

$$\ln \eta(x) = -1 + \sum_{k=0}^{N} \lambda_k x^k \xrightarrow{\frac{\partial(\ln \eta(x))}{\partial x}} \eta(x) = e^{-1+\sum_{k=1}^{N} \lambda_k x^k} = e^{\sum_{k=0}^{N} \lambda_k x^k} \tag{3.4}$$

To calculate the solution of the maximum entropy method, one has to solve for the Lagrange multipliers λ_k. The only way to do so is to solve the following system of non linear equations,

$$\begin{aligned} &\int_\Omega e^{\lambda_0+\lambda_1 x+\ldots+\lambda_k x^k}\,dx = \mu_0, \\ &\int_\Omega x e^{\lambda_0+\lambda_1 x+\ldots+\lambda_k x^k}\,dx = \mu_1, \\ &\qquad\ldots \\ &\int_\Omega x^k e^{\lambda_0+\lambda_1 x+\ldots+\lambda_k x^k}\,dx = \mu_k \end{aligned} \tag{3.5}$$

In the current thesis we utilize MATLAB and Python built in solvers for nonlinear systems, in order to solve the nonlinear system of equations. The Jacobian can also be calculated; if one denotes the moments based on the maximum entropy solution as,

$$\tilde{\mu}_k = \int_\Omega x^k e^{\lambda_0+\lambda_1 x+\ldots+\lambda_k x^k}\,dx \tag{3.6}$$

then the Jacobian matrix is calculated as follows,

$$J = \begin{bmatrix} \frac{\partial\tilde{\mu}_0}{\partial\lambda_0} & \frac{\partial\tilde{\mu}_0}{\partial\lambda_1} & \ldots & \frac{\partial\tilde{\mu}_0}{\partial\lambda_k} \\ \frac{\partial\tilde{\mu}_1}{\partial\lambda_0} & \frac{\partial\tilde{\mu}_1}{\partial\lambda_1} & \ldots & \frac{\partial\tilde{\mu}_1}{\partial\lambda_k} \\ \frac{\partial\tilde{\mu}_2}{\partial\lambda_0} & \frac{\partial\tilde{\mu}_2}{\partial\lambda_1} & \ldots & \frac{\partial\tilde{\mu}_2}{\partial\lambda_k} \\ \ldots & \ldots & \ldots & \ldots \\ \frac{\partial\tilde{\mu}_k}{\partial\lambda_0} & \frac{\partial\tilde{\mu}_k}{\partial\lambda_1} & \ldots & \frac{\partial\tilde{\mu}_k}{\partial\lambda_k} \end{bmatrix} = \begin{bmatrix} \tilde{\mu}_0 & \tilde{\mu}_1 & \ldots & \tilde{\mu}_k \\ \tilde{\mu}_1 & \tilde{\mu}_2 & \ldots & \tilde{\mu}_{k+1} \\ \tilde{\mu}_2 & \tilde{\mu}_3 & \ldots & \tilde{\mu}_{k+2} \\ \ldots & \ldots & \ldots & \ldots \\ \tilde{\mu}_k & \tilde{\mu}_{k+1} & \ldots & \tilde{\mu}_{k+k} \end{bmatrix} \tag{3.7}$$

In the above equation $\tilde{\mu}_k$ is the k^{th} moment of the reconstructed distribution, thus the Newton solver is going to find λ_k when $\left\|\tilde{\mu}_k - \mu_k\right\|$ is below a specified tolerance.

In order to solve the prescribed problem initial values are mandatory. It has been tested and proven that because of problem's sensitivity the proper initial values for Gaussian like distributions are the following,

$$\lambda_i^{initial} = \begin{cases} -\ln\sqrt{2\pi}, & i = 0 \\ 0, & \text{otherwise} \end{cases} \tag{3.8}$$

These guesses are all based in Gaussian distribution with ($\mu = 0, \sigma = 1$). In this diploma thesis Py Max Ent and Mat Max Ent codes have been used for the reconstruction of the chosen initial function.

Mat Max Ent – Py Max Ent

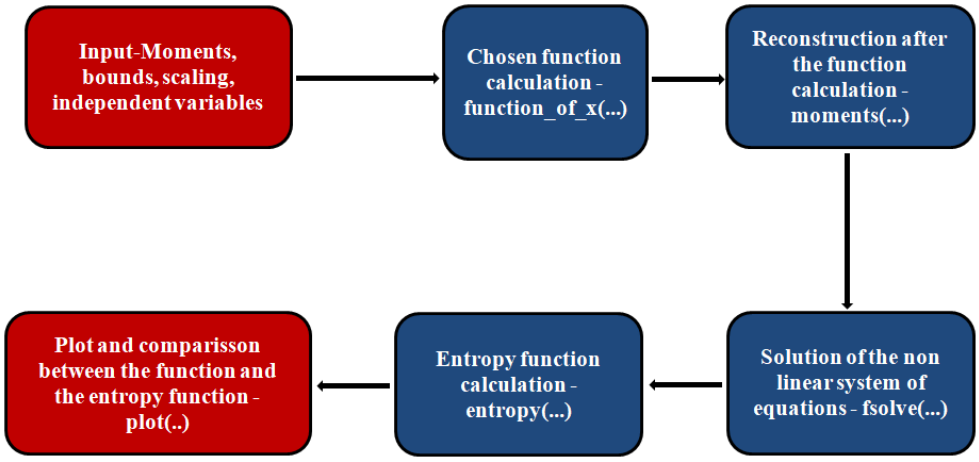

Figure 3.1. Flowchart of Mat Max Ent code.

Mat Max Ent is a code written in MATLAB and it is the basic tool that has been used in order to achieve the reconstruction of the density function given a small set of low order moments, produce smoother density functions and make the comparison with the solutions of the CPB problem with the finite elements method.

The only way to reach the final result is using the algorithm above. The results have all been rechecked being compared to those of the Py Max Ent algorithm that follows. Figure 3.1 illustrates the flowchart of the Mat Max Ent code written in MATLAB.

The inputs of this code are, the moments, the boundaries and the total points that the researcher decides to discretize the domain over x axis (1D). Next, follows the choice of a function, its boundaries, a resolution for the domain (discretization points) and its moments.

Solution of the nonlinear system of equations is achieved using the fsolve function of MATLAB or Python and having as input data the moments and the boundary conditions of the problem. The final steps of the flowchart are the calculation of the maximum entropy function and the comparison between the maximum entropy function and the initial function of the problem.

During the calculation of the maximum entropy function one has already calculated the Lagrangian multipliers after the solution of the nonlinear system of equations and uses the Lagrangian multipliers and the values over the x domain as input for the exact calculation of the maximum entropy function. As far as the comparison is concerned, it is achieved doing both the plots of the maximum entropy function and the (original) function of the problem.

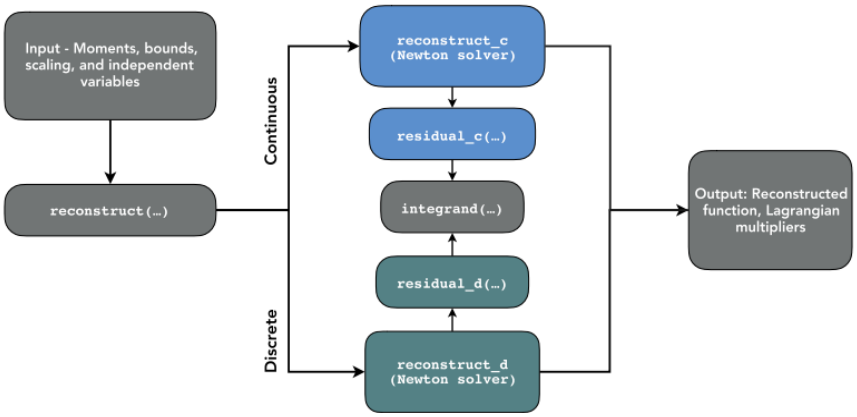

Figure 3.2. Flowchart of Py Max Ent code.

Figure 3.2 shows the flowchart of the Py Max Ent code written in Python. The whole procedure is quite similar to that of Mat Max Ent, as the basic steps of calculation are similar. The Py Max Ent code goes from the reconstruction to the Newton solver. Next follows the calculation of the residual c or the residual d, where the residual c function calculates the integrated right hand side of the moment approximation function, in case that one studies a continuous (original) function and the residual d function calculates the integrated right hand side of the moment approximation function, in case that one studies a discrete (original) function, followed by the integration of the inner product of domain x and reconstructed moments. The final step is the comparison between entropy and the chosen (original) function.

The software is written in Python due to its popularity and ease of use in addition to the availability of a robust multidimensional nonlinear solver through SciPy. The Py Max Ent code offers a single interface to both the continuous and discrete maximum entropy reconstructions along with a few useful functions described below.

The implementation of Py Max Ent is very simple and takes form in a single Python file called pymaxent.py. For proper operation, three separate helper routines are implemented for the continuous and for the discrete case. These are a numerical integrator, a residual error calculator, and a Newton solver as shown in Figure 3.2. The Newton solver is based on SciPy's multidimensional root finding routine, fsolve. From the user's perspective, a single function call is made to the main routine, reconstruct (discussed below).

To use Py Max Ent, a single call to the function reconstruct is needed. Here, moments is a required list or array of known moments, rndvar is an optional argument containing discrete values of the random variable, and bnds is a tuple [a,b] containing the expected bounds of the resulting distribution. When rndvar is provided, the reconstruction assumes a discrete distribution. The code returns two quantities: (1) the functional form of the solution, which can be plotted and, (2) a numpy array containing the Lagrangian multipliers. In the discrete case, the functional solution is simply a numpy array of values containing the function values. Finally, Py Max Ent provides a helper routine named moments that calculates the first k moments of a function and is useful for verification purposes **(Saad and Ruai 2019)**.

3.3 Maximum entropy method results and comparison

The comparison between the Mat Max Ent code and the Py Max Ent code is presented below. More analytically, two benchmark cases are presented. In the first case a unimodal initial function has been chosen, whereas in the second case a bimodal initial function has been studied. The basic purpose is to reconstruct the maximum entropy function and make the comparison with the exact solution.

3.3.1 Unimodal Case

The chosen for reconstruction initial unimodal function is calculated from the following formula and it is the same for all the following unimodal examples.

$$f(x)=\frac{1}{2\sigma_0\sqrt{2\pi}}\frac{e^{-(x-\mu)^2}}{2\sigma^2} \qquad (3.9)$$

The reconstructed maximum entropy function compared to the initial unimodal function and the comparison between the Py Max Ent code and the Mat Max Ent code are shown below. Both solutions converge to the exact one, but one can observe that when the user increases the number of moments the error between the exact and the reconstructed solution becomes even smaller. Theoretically, the user can use an infinite number of moments, but in practice the algorithm requires only a small number of low order moments in order to reconstruct the original function as it appears in the figure below.

Domain [-2,2]

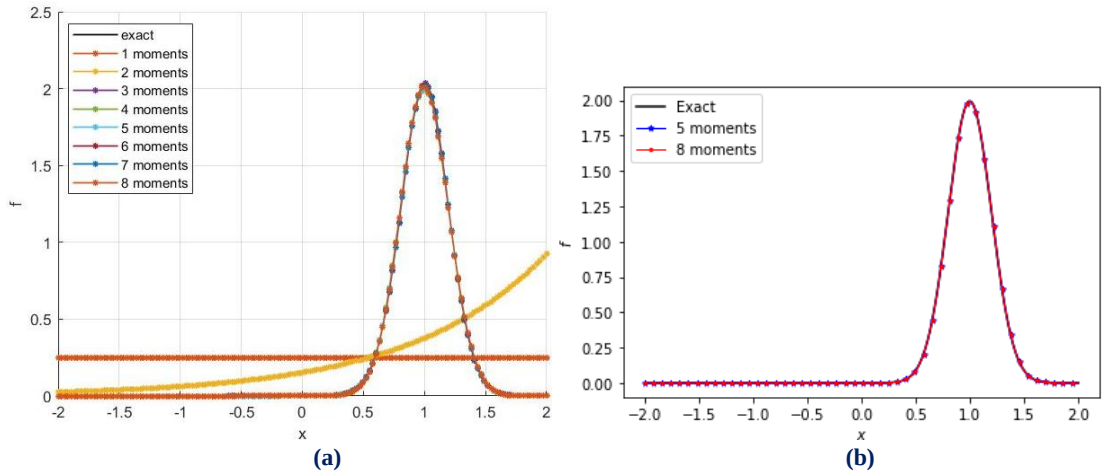

(a) **(b)**

Figure 3.3. Reconstructed entropy function, domain [-2,2], using
(a) Mat Max Ent for different number of moments,
(b) Py Max Ent for eight and five moments.

Figure 3.3 presents the maximum entropy function using **(a)** the Mat Max Ent code and **(b)** the Py Max Ent code. The figure presents the maximum entropy function and shows the comparison between the two codes, in case that one uses from one to eight finite moments.

Domain [0,2]

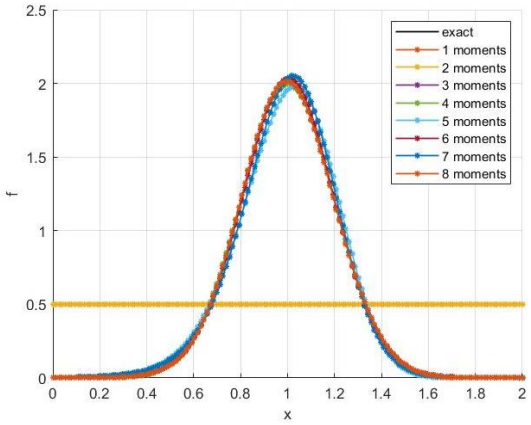

(a)

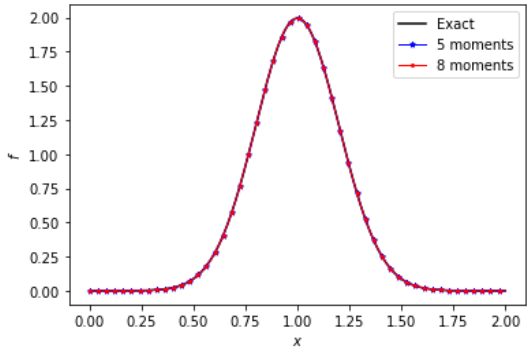

(b)

Figure 3.4. Reconstructed maximum entropy function, domain [0,2], using
(a) Mat Max Ent for different number of moments,
(b) Py Max Ent for eight and five moments.

Figure 3.4 presents the reconstructed unimodal chosen function and shows **(a)** the Mat Max Ent code using one to eight moments compared to the exact solution and **(b)** the Py Max Ent code for five and eight moments in comparison with the exact solution.

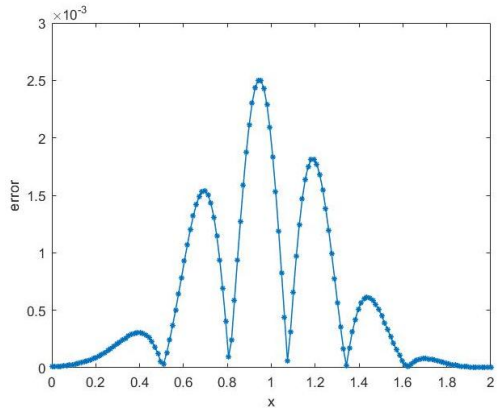

Figure 3.5. Reconstructed maximum entropy function error, domain [0,2], for eight moments using Mat Max Ent.

Figure 3.5 presents the error over the x axis between the exact solution and the reconstructed maximum entropy function with eight moments using the Mat Max Ent code.

Domain [0,4]

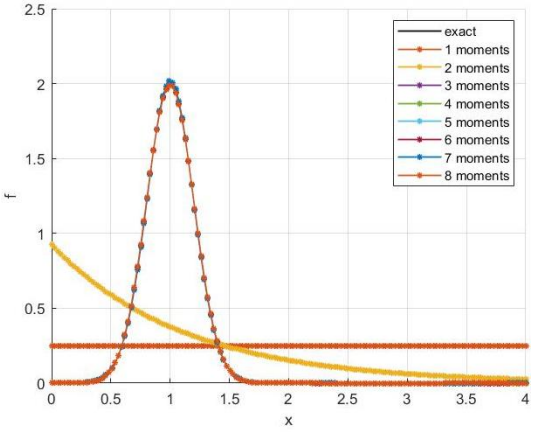

(a)

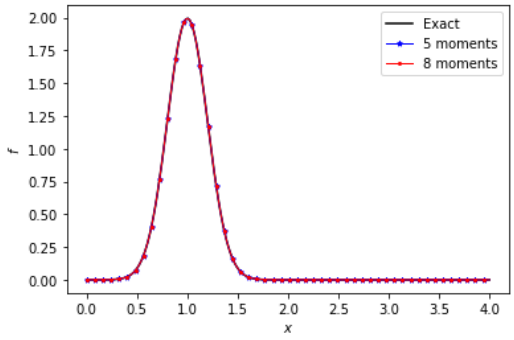

(b)

Figure 3.6. Reconstructed entropy function, domain [0,4], using
(a) Mat Max Ent for different number of moments,
(b) Py Max Ent for eight and five moments.

Figure 3.6 shows the reconstructed unimodal function (Eq. 3-9) and shows **(a)** the Mat Max Ent code results using one to eight moments, and the comparison with the exact solution and **(b)** the Py Max Ent code for five and eight moments, and its comparison with the exact solution.

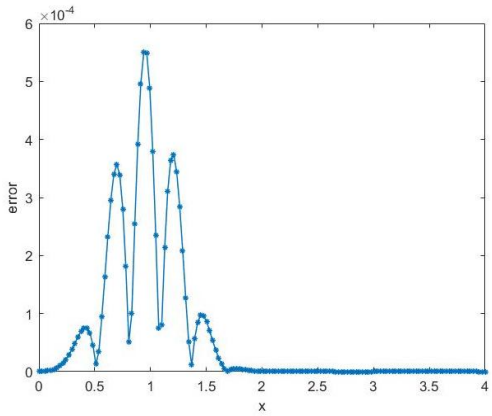

Figure 3.7. Reconstructed maximum entropy function error, domain [0,4], for eight moments using Mat Max Ent.

Figure 3.7 presents the error over the x axis between the exact solution and the reconstructed entropy function with eight moments using the Mat Max Ent code.

3.3.2 Bimodal case

In statistics a multimodal distribution is a probability distribution with more than one peaks or “modes” which may also be referred to as a bimodal distribution, when we talk about a distribution with two peaks. These appear as distinct peaks (local maxima) in the probability density function. Mathematically a bimodal distribution most commonly arises as a mixture of two different unimodal distributions.

The chosen function for reconstruction initial bimodal f is calculated from the following formula and it is the same for all the following bimodal examples.

$$f(x)=\frac{1}{2\sigma_0\sqrt{2\pi}}e^{-\frac{(x-\mu_0)^2}{2\sigma_0^2}}+\frac{1}{2\sigma_1\sqrt{2\pi}}e^{-\frac{(x-\mu_1)^2}{2\sigma_1^2}} \qquad (3.10)$$

Domain [-1,1]

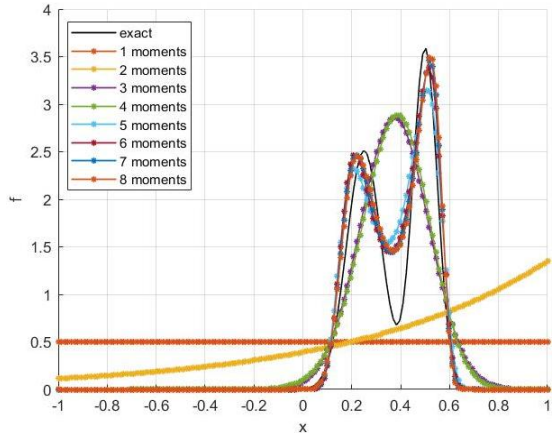

(a)

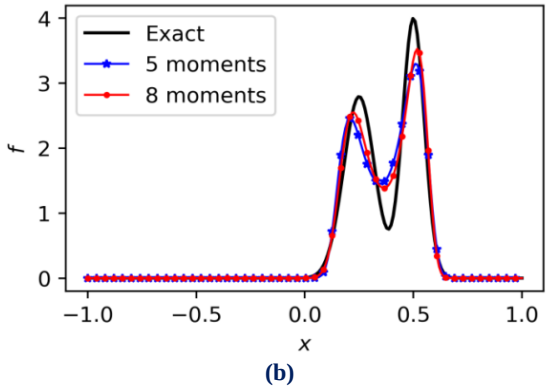

(b)

Figure 3.8. Reconstructed maximum entropy function, domain [-1,1], using
(a) Mat Max Ent for different number of moments,
(b) Py Max Ent for eight and five moments.

Figure 3.8 illustrates the reconstructed bimodal function (Eq. 3-10) and shows **(a)** the Mat Max Ent code results using one to eight moments compared to the exact solution and **(b)** the Py Max Ent code for five and eight moments in comparison with the exact solution.

Domain [0,1]

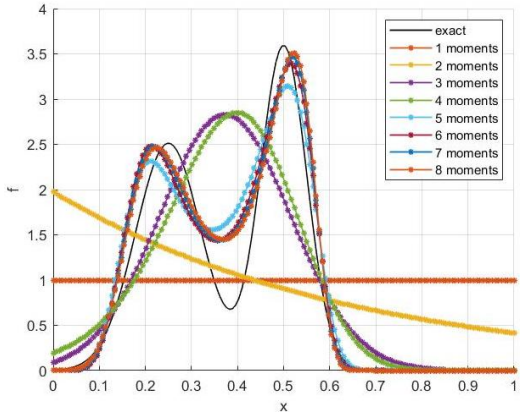

(a)

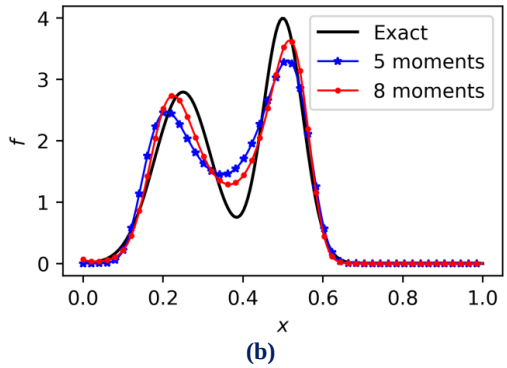

(b)

Figure 3.9. Reconstructed maximum entropy function, domain [0,1], using
(a) Mat Max Ent for different number of moments,
(b) Py Max Ent for eight and five moments.

Figure 3.9 shows the reconstructed bimodal function (Eq. 3-10) and depicts **(a)** the Mat Max Ent code results using one to eight moments, its comparison against the exact solution and **(b)** the Py Max Ent code results for five and eight moments, and its comparison with the exact solution.

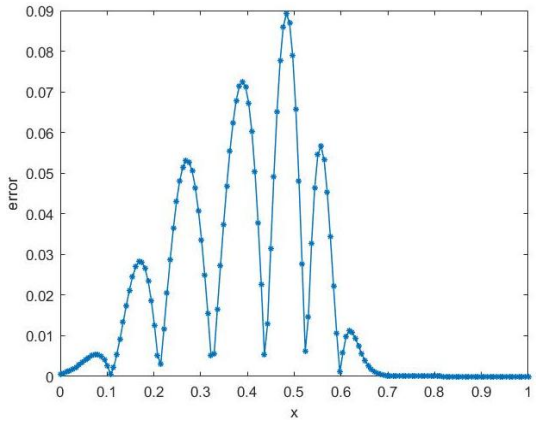

Figure 3.10. Reconstructed maximum entropy function error, domain [0,1], for eight moments using Mat Max Ent.

Figure 3.10 presents the error over the x axis between the exact solution and the reconstructed entropy function with eight moments using the Mat Max Ent code.

Domain [0,2]

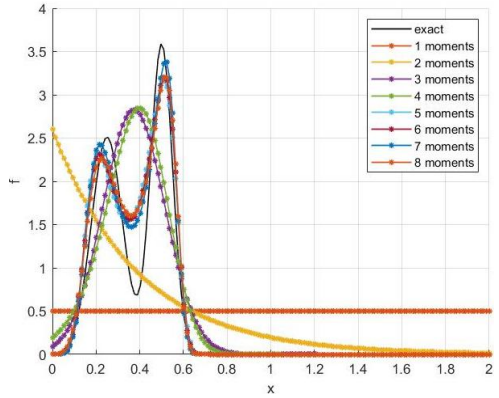

(a)

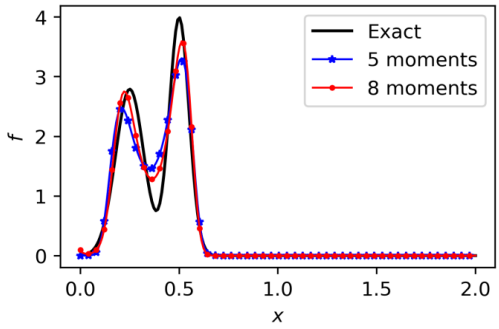

(b)

Figure 3.11. Reconstructed maximum entropy function, domain [0,2], using
(a) Mat Max Ent for different number of moments,
(b) Py Max Ent for eight and five moments.

Figure 3.11 illustrates the reconstructed bimodal function and depicts **(a)** the Mat Max Ent code using one to eight moments, original function given from (Eq.3-10) and **(b)** the Py Max Ent code for five and eight moments, and its comparison with the original function.

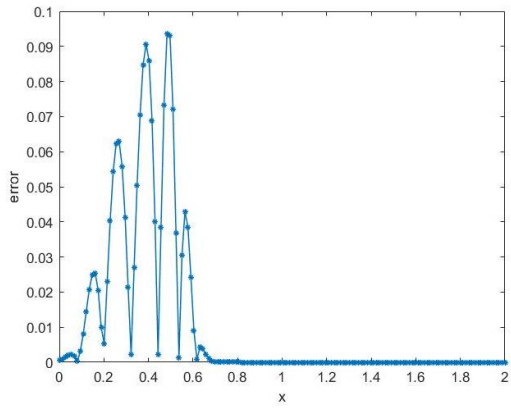

Figure 3.12. Reconstructed maximum entropy function error, domain [0,1], for eight moments using Mat Max Ent.

Figure 3.10 shows the error over the x axis between the exact solution and the reconstructed maximum entropy function with eight moments using the Mat Max Ent code.

4 Results

4.1 Introduction

In this chapter we present the results of the solution of the population balance equations using the maximum entropy method of moments. The maximum entropy method of moments is compared against the finite elements method. The basic goal is to solve the non linear system of partial-integro-differential equations reducing the computational cost. This is achieved by using the maximum entropy method of moments, because one goes from a system with a few thousands of equations (resulting in from the discretization of the partial-integro-differential equations), to a system much simpler to solve, with a number of equations equal to the number of the chosen moments. The basic question was, is it even possible to capture accurately the density function by evolving only a few equations for the moments evolution? All the codes are written in and the research was made making use of the commercial software MATLAB R2020b and Spyder 5.0.0. The simulations were performed in Windows environment.

4.2 CPB problem expressed with moments

CPB expressed in the physical domain - discrete partitioning

Given the expressions (2.17), (2.18), and (2.19), the CPB model for isogenic populations which carry the Lac Operon gene regulatory network reads:

$$\frac{\partial n}{\partial t}+\frac{\partial(R(\mathrm{x})n(x,t))}{\partial x}+\left(\frac{x}{\langle x\rangle}\right)^{m} n(x,t)=\frac{1}{f}\left(\frac{x}{f\langle x\rangle}\right)^{m} n\left(\frac{x}{f},t\right)+\ldots$$
$$\frac{1}{1-f}\left(\frac{x}{(1-f)\langle x\rangle}\right)^{m} n\left(\frac{x}{1-f},t\right)-n(\mathrm{x},t)\int_{0}^{x\max}\left(\frac{x}{\langle x\rangle}\right)^{m} n(\mathrm{x},t)\,dx \qquad (4.1)$$

Multiplying both terms of the equations with the term x^k and integrating the expression (4.1) from zero to $x_{\max}$, the desirable expression of the method of moments is received, as follows:

$$\int_{0}^{\infty}\frac{\partial n}{\partial t}x^{k}dx+\int_{0}^{\infty}\frac{\partial(R(\mathrm{x})n(x,t))}{\partial x}x^{k}dx+\int_{0}^{\infty}\left(\frac{x}{\langle x\rangle}\right)^{m} n(x,t)\,x^{k}dx=\ldots$$
$$\int_{0}^{\infty}\frac{1}{f}\left(\frac{x}{f\langle x\rangle}\right)^{m} n\left(\frac{x}{f},t\right)x^{k}dx+\ldots$$
$$\int_{0}^{\infty}\frac{1}{1-f}\left(\frac{x}{(1-f)\langle x\rangle}\right)^{m} n\left(\frac{x}{1-f},t\right)x^{k}dx-\ldots$$
$$\int_{0}^{\infty} n(\mathrm{x},t)\,x^{k}\int_{0}^{x\max}\left(\frac{x}{\langle x\rangle}\right)^{m} n(\mathrm{x},t)\,dxdx \qquad (4.2)$$

Since $\int_0^{\infty} \frac{\partial n x^k}{\partial t} dx = \frac{d\mu_k}{dt}$, it follows that the expression (4.2) receives the following form,

$$\frac{d\mu_k}{dt} + \left| R(\mathrm{x}) n(x,t) x^k \right|_0^{\infty} - \int_0^{\infty} R(\mathrm{x}) n(x,t) k x^{k-1} dx + \int_0^{\infty} \left(\frac{x}{\langle x \rangle} \right)^m n(x,t) x^k dx = \ldots$$
$$\int_0^{\infty} \left\{ \begin{array}{l} \left(\frac{x}{\langle x \rangle} \right)^m x^k \left[\frac{1}{f^{m+1}} n\left(\frac{x}{f}, t \right) + \frac{1}{(1-f)^{m+1}} n\left(\frac{x}{1-f}, t \right) \right] - \ldots \\ n(x,t) x^k \int_0^{x\max} \left(\frac{x}{\langle x \rangle} \right)^m n(x,t) dx \end{array} \right\} \quad (4.3)$$

CPB expressed in the normalized domain - discrete partitioning

Equation 4.3 is used when one works in the physical domain, while for the normalized domain the researcher can follow the same steps, but Equation 4.1 is changed and the particular CPB problem is formulated as follows. In order to confront with the problem of the unknown boundary for the intracellular content, we first normalize the physiological state space with respect to the average intracellular content $\langle x \rangle$,

$$0 \le x \le x_{\max} \Rightarrow 0 \le \frac{x}{\langle x \rangle} \le \frac{x_{\max}}{\langle x \rangle} = z_{\max} \Rightarrow 0 \le \frac{x}{\langle x \rangle z_{\max}} \le 1 \quad (4.4)$$

First the transformed density function $g(\xi, t)$ is defined as,

$$n(x,t)\,\mathrm{dx} = g(\xi,t)\, d\xi \quad (4.5)$$

and differentiating (4.5) with respect to time and combining with (3.1) we derive the following relation for the time derivative of $n(x,t)$,

$$\frac{dn}{dt} = \frac{1}{z_{\max}} \left[\frac{dg}{dt} - \frac{1}{\langle x \rangle} \frac{d\langle x \rangle}{dt} \frac{\partial(\xi g)}{\partial \xi} \right] \quad (4.6)$$

From (4.1), (4.4), (4.5) and (4.6) the transformed density functions is calculated as,

$$\frac{\partial g(\xi,\mathrm{t})}{\partial t} - \frac{1}{\langle x \rangle} \frac{\partial \langle x \rangle}{\partial t} \frac{\partial(\xi\, \mathrm{g}(\xi,t))}{\partial x} + \frac{1}{\langle x \rangle z_{\max}} \frac{\partial \left[\overline{R}\, \mathrm{g}(\xi,t) \right]}{\partial \xi} = \ldots$$
$$z_{\max}^m \left[\frac{1}{f} \gamma\left(\frac{\xi}{f} \right) g\left(\frac{\xi}{f}, t \right) + \frac{1}{1-f} \gamma\left(\frac{\xi}{1-f} \right) g\left(\frac{\xi}{1-f}, t \right) - \gamma(\xi) g(\xi,t) \right] \ldots$$
$$- z_{\max}^m g(\xi,t) \int_0^1 \gamma(\xi) g(\xi,t) d\xi \quad (4.7)$$

Taking the first-order moment of (4.1) and applying conservation of mass for the intracellular component at cell division, leads to the equation,

$$\frac{d\langle x\rangle}{dt}=\int_0^1 R(\xi)g(\xi,\mathrm{t})\,d\xi-\langle x\rangle\int_0^1\Gamma(\xi)g(\xi,\mathrm{t})\,d\xi \qquad (4.8)$$

Now that the first order moment is transformed, one needs to multiply both parts of the equation with the term ξ^k , then integrate from zero to one and consequently (4.7) receives its final form.

$$\begin{aligned}&\int_0^1\frac{\partial g(\xi,\mathrm{t})}{\partial t}\xi^k d\xi+\int_0^1\frac{\partial\left(\xi g(\xi,\mathrm{t})\right)}{\partial\xi}\xi^k\frac{1}{\langle x\rangle}\int_0^1\overline{R}(\xi)\,\mathrm{g}(\xi,t)d\xi d\xi-\ldots\\&\int_0^1\frac{\partial\left(\xi g(\xi,\mathrm{t})\right)}{\partial\xi}\xi^k z_{\max}^m\int_0^1\gamma(\xi)\,g(\xi,t)\,d\xi d\xi+\int_0^1\frac{1}{\langle x\rangle z_{\max}}\frac{\partial\left(\overline{R}(\xi)g(\xi,\mathrm{t})\right)}{\partial\xi}\xi^k d\xi=\ldots\\&\int_0^1 z_{\max}^m\left[\frac{1}{f}\gamma\left(\frac{\xi}{f}\right)g\left(\frac{\xi}{f},t\right)+\frac{1}{1-f}\gamma\left(\frac{\xi}{1-f}\right)g\left(\frac{\xi}{1-f},t\right)-\gamma(\xi)\,g(\xi,t)\right]\xi^k\,\mathrm{d}\,\xi-\ldots\\&-\int_0^1 z_{\max}^m g(\xi,t)\,\xi^k\int_0^1\gamma(\xi)\,g(\xi,t)\,d\xi d\xi\end{aligned} \qquad (4.9)$$

After both parts of the equation are multiplied by ξ^k, follows the observation that $\int_0^1\frac{\partial g\xi^k}{\partial t}dx=\frac{d\mu_k}{dt}$ and consequently expression (4.9) receives its final form,

$$\begin{aligned}&\frac{\partial\mu_k}{\partial t}=-\left|\xi g(\xi,\mathrm{t})\xi^k\frac{1}{\langle x\rangle}\int_0^1\overline{R}(\xi)\,\mathrm{g}(\xi,t)\,d\xi\right|_0^1+\ldots\\&\int_0^1\xi\,\mathrm{g}(\xi,t)\left(k\xi^{k-1}\frac{1}{\langle x\rangle}\int_0^1\overline{R}(\xi)\,\mathrm{g}(\xi,t)\,d\xi+\xi^k\frac{1}{\langle x\rangle}\overline{R}(\xi)\,\mathrm{g}(\xi,t)\right)+\ldots\\&\left|\xi g(\xi,\mathrm{t})\xi^k z_{\max}^m\int_0^1\gamma(\xi)\,\mathrm{g}(\xi,t)\,d\xi\right|_0^1-\ldots\\&\int_0^1\xi\,\mathrm{g}(\xi,t)\left(k\xi^{k-1}z_{\max}^m\int_0^1\gamma(\xi)\,\mathrm{g}(\xi,t)\,d\xi+\xi^k z_{\max}^m\gamma(\xi)\,\mathrm{g}(\xi,t)\right)-\ldots\\&\frac{1}{\langle x\rangle z_{\max}}\left|\overline{R}(\xi)g(\xi,\mathrm{t})\xi^k\right|_0^1+\frac{1}{\langle x\rangle z_{\max}}\int_0^1\overline{R}(\xi)g(\xi,\mathrm{t})\,\mathrm{k}\,\xi^{k-1}d\xi+\ldots\\&\int_0^1 z_{\max}^m\left[\frac{1}{f}\gamma\left(\frac{\xi}{f}\right)g\left(\frac{\xi}{f},t\right)+\frac{1}{1-f}\gamma\left(\frac{\xi}{1-f}\right)g\left(\frac{\xi}{1-f},t\right)-\gamma(\xi)\,g(\xi,t)\right]\xi^k\,\mathrm{d}\,\xi-\ldots\\&-\int_0^1 z_{\max}^m g(\xi,t)\,\xi^k\int_0^1\gamma(\xi)\,g(\xi,t)\,d\xi d\xi\end{aligned} \qquad (4.10)$$

CPB expressed using symmetric partitioning

The number density function dynamics are expressed as follows,

$$\frac{\partial n}{\partial t}+\frac{\partial(R(\mathrm{x})n(x,t))}{\partial x}+\Gamma(x)n(x,t)=\ldots$$
$$2\int_{x}^{x_{\max}}\Gamma(y)P(x,\mathrm{y})n(\mathrm{y},t)\,dy-n(\mathrm{x},t)\int_{0}^{x\max}\Gamma(x)n(x,t)\,dx \qquad (4.11)$$

Equation (4.11) is formulated for the fixed normalized domain $\xi\in[0,1]$, where $\xi=\frac{x}{x_{\max}}$,

$$n(x,t)\,dx=n(\xi,t)\,d\xi\Rightarrow n(x,t)\,x_{\xi}=\hat{n}(\xi,\tau)\Rightarrow\ldots$$
$$n(x,t)\,x_{\max}=\hat{n}(\xi,\tau) \qquad (4.12)$$

and differentiating with respect to τ,

$$\frac{\partial\left(n(x,t)\,x_{\max}\right)}{\partial\tau}=\frac{\partial\left(\hat{n}(\xi,\tau)\right)}{\partial\tau}\Rightarrow\ldots$$
$$x_{\max}\left(\frac{\partial n}{\partial x}\frac{\partial x}{\partial\tau}+\frac{\partial n}{\partial\tau}\right)+n\frac{\partial x_{\max}}{\partial\tau}=\frac{\partial\hat{n}}{\partial\tau}\Rightarrow\ldots$$
$$x_{\max}\left(\frac{\partial\left(x_{\max}\right)^{-1}\hat{n}}{\partial\xi}\left(x_{\max}\right)^{-1}\frac{\partial\left(\xi x_{\max}\right)}{\partial\tau}+\frac{\partial n}{\partial\tau}\right)+\left(x_{\max}\right)^{-1}\hat{n}\frac{\partial x_{\max}}{\partial\tau}=\frac{\partial\hat{n}}{\partial\tau}\Rightarrow\ldots$$
$$x_{\max}\left[\frac{\partial x_{\max}}{\partial\tau}\left(x_{\max}\right)^{-1}\frac{\partial\hat{n}}{\partial\xi}\xi+\frac{\partial n}{\partial\tau}\right]+\left(x_{\max}\right)^{-1}\hat{n}\frac{\partial x_{\max}}{\partial\tau}=\frac{\partial\hat{n}}{\partial\tau}\Rightarrow\ldots$$
$$\frac{1}{x_{\max}}\frac{\partial x_{\max}}{\partial\tau}\left[\frac{\partial\hat{n}}{\partial\xi}\xi+\hat{n}\right]+x_{\max}\frac{\partial n}{\partial\tau}=\frac{\partial\hat{n}}{\partial\tau}\Rightarrow\ldots$$
$$\frac{\partial\hat{n}}{\partial\tau}=\frac{1}{x_{\max}}\frac{\partial\hat{n}}{\partial\tau}-\frac{1}{x^{2}}\frac{\partial x_{\max}}{\partial\tau}\frac{\partial\left(\xi\hat{n}\right)}{\partial\xi} \qquad (4.13)$$

The formulation of the reaction rate R(x) in terms of the new variable ξ, e.g. if.

$$R(x)=\frac{\pi p+x^{2}}{p+x^{2}}-\delta x\Rightarrow\ldots$$
$$\hat{R}(\xi)=\frac{\pi p+\left[\xi x_{\max}\right]^{2}}{p+\left[\xi x_{\max}\right]^{2}}-\delta\left[\xi x_{\max}\right]\Rightarrow\ldots$$
$$\frac{\partial\left(R(x)n\right)}{\partial x}=\frac{\partial\left(\hat{R}(\xi)\frac{1}{x_{\max}}\hat{n}\right)}{\partial\xi}\frac{1}{x_{\max}}=\frac{\partial\left(\hat{R}(\xi)\hat{n}\right)}{\partial\xi}\frac{1}{x_{x_{\max}}^{2}} \qquad (4.14)$$

The division rate is given by,

$$\Gamma(x)=x^{L}\Rightarrow\Gamma(\xi)=\left(\xi x_{\max}\right)^{L}\Rightarrow\Gamma(x)n=\hat{\Gamma}(\xi)\hat{n}\frac{1}{x_{\max}} \qquad (4.15)$$

if the partition probability density function is given by,

$$P(x,y)=\frac{1}{y}\frac{\Gamma amma(2q+2)}{\Gamma amma(q+1)\Gamma amma(q+1)}\left(\frac{x}{y}\right)^q\left(1-\frac{x}{y}\right)^q \xrightarrow{\psi=\frac{y}{x_{\max}}}\ldots$$
$$P(\xi,\psi)=\frac{1}{x_{\max}}\frac{1}{\psi}\frac{\Gamma amma(2q+2)}{\Gamma amma(q+1)\Gamma amma(q+1)}\left(\frac{\xi}{\psi}\right)^q\left(1-\frac{\xi}{\psi}\right)^q \quad (4.16)$$

Following,

$$2\int_x^{x_{\max}}\Gamma(y)P(x,y)n(y)dy=2\int_\xi^1\hat{\Gamma}(\psi)P(\xi,\psi)\hat{n}(\psi)d\psi \quad (4.17)$$

and the dilution term,

$$n\int_0^{x_{\max}}\Gamma(y)n(y)dy=\frac{1}{x_{\max}}\hat{n}\int_0^1\hat{\Gamma}(\psi)\hat{n}(\psi)d\psi \quad (4.18)$$

The derivation of the dynamics of $\hat{n}$ is given by,

$$\frac{1}{x_{\max}}\frac{\partial\hat{n}}{\partial\tau}-\frac{1}{x_{x_{\max}}^2}\frac{\partial x_{\max}}{\partial\tau}\frac{\partial(\xi\hat{n})}{\partial\xi}+\frac{\partial\left(\hat{R}(\xi)\hat{n}\right)}{\partial\xi}\frac{1}{x_{x_{\max}}^2}+\hat{\Gamma}(\xi)\hat{n}\frac{1}{x_{\max}}=\ldots$$
$$2\int_\xi^1\hat{\Gamma}(\psi)\hat{P}(\xi,\psi)\hat{n}(\psi)d\psi-\frac{1}{x_{\max}}\hat{n}\int_0^1\hat{\Gamma}(\psi)\hat{n}(\psi)d\psi\Leftrightarrow\ldots$$
$$\frac{\partial\hat{n}}{\partial\tau}=\frac{1}{x_{\max}}\frac{\partial x_{\max}}{\partial\tau}\frac{\partial(\xi\hat{n})}{\partial\xi}-\frac{\partial\left(\hat{R}(\xi)\hat{n}\right)}{\partial\xi}\frac{1}{x_{\max}}-\hat{\Gamma}(\xi)\hat{n}+\ldots \quad (4.19)$$
$$2x_{\max}\int_\xi^1\hat{\Gamma}(\psi)\hat{P}(\xi,\psi)\hat{n}(\psi)d\psi-\hat{n}\int_0^1\hat{\Gamma}(\psi)\hat{n}(\psi)d\psi$$

Multiplying both terms of the equations with the term x^k and integrating the expression (4.7) from zero to $x_{\max}$, the desirable expression of the method of moments is received, as follows.

$$\int_0^{x_{\max}}\frac{\partial n}{\partial t}x^k+\left|R(\mathrm{x})n(x,t)x^k\right|_0^{x_{\max}}-\int_0^{x_{\max}}R(\mathrm{x})n(x,t)kx^{k-1}dx+\int_0^{x_{\max}}\Gamma(x)n(x,t)x^kdx=\ldots$$
$$\int_0^{x_{\max}}2x^k\int_x^{x_{\max}}\Gamma(y)P(x,\mathrm{y})n(\mathrm{y},t)dydx-\ldots$$
$$\int_0^{x\max}n(\mathrm{x},t)x^k\int_0^{x\max}\Gamma(x)n(x,t)dxdx\xrightarrow{\int_0^{x_{\max}}\frac{\partial nx^k}{\partial t}dx=\frac{\partial\mu_k}{\partial t}\ \&\ \int_0^{x_{\max}}R(\mathrm{x})n(x,t)kx^{k-1}dx=0}\ldots$$
$$\frac{\partial\mu_k}{\partial t}=\int_0^{x_{\max}}R(\mathrm{x})n(x,t)kx^{k-1}dx-\int_0^{x_{\max}}\Gamma(x)n(x,t)x^kdx+\ldots \quad (4.20)$$
$$\int_0^{x_{\max}}2x^k\int_x^{x_{\max}}\Gamma(y)P(x,\mathrm{y})n(\mathrm{y},t)dydx-\int_0^{x\max}n(\mathrm{x},t)x^k\int_0^{x\max}\Gamma(x)n(x,t)dxdx$$

4.3 Numerical solution of the CPB problem

4.3.1 Discrete partitioning

As far as the results of this diploma thesis is concerned, simulations with the maximum entropy method of moments are performed for various parameter values of f and p and compare the results against a finite element code which was implemented in **(Kavousanakis et al. 2009)** using COMSOL Multiphysics software. The results of a transient simulation of the system of equations subject to the boundary conditions: **(a)** $n(0,t)=n(\mathrm{x}_{\max},t)=0$ for the case that one solves the CPB problem in the physical domain and **(b)** $g(0,t)=g(1,t)=0$ for the case that one solves the CPB problem in the normalized domain are thoroughly presented and explained.

The results of a transient simulation of the system of equations of isogenic cell population with Lac Operon genetic network are depicted in Figure 4.1. for the following parameter values: $f=0.40$, $m=3$, $p=0.05$, $\pi=0.03$, $\delta=0.05$, $z_{\max}=4$.

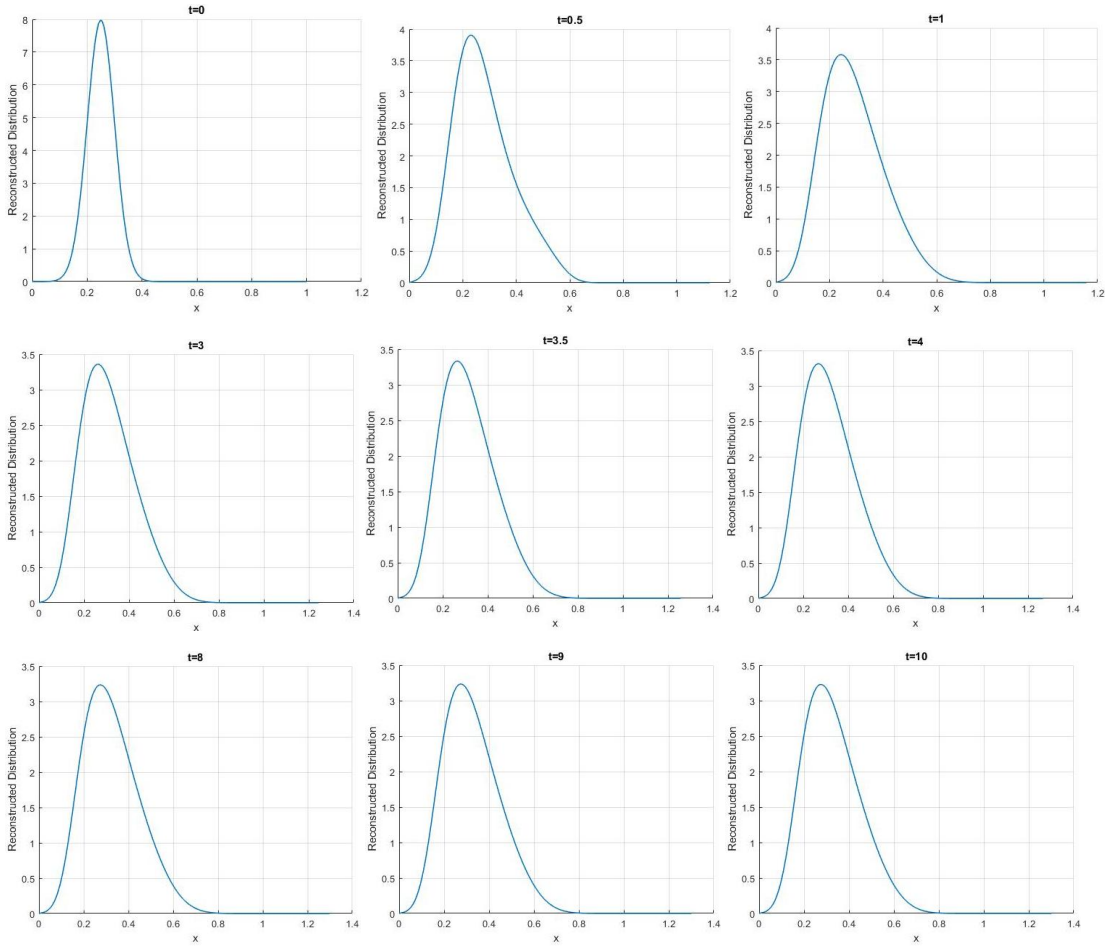

Figure 4.1. Simulation of a cell population using the maximum entropy method of moments in the physical domain. Parameter values:
f=0.40, p=0.05, m=3.

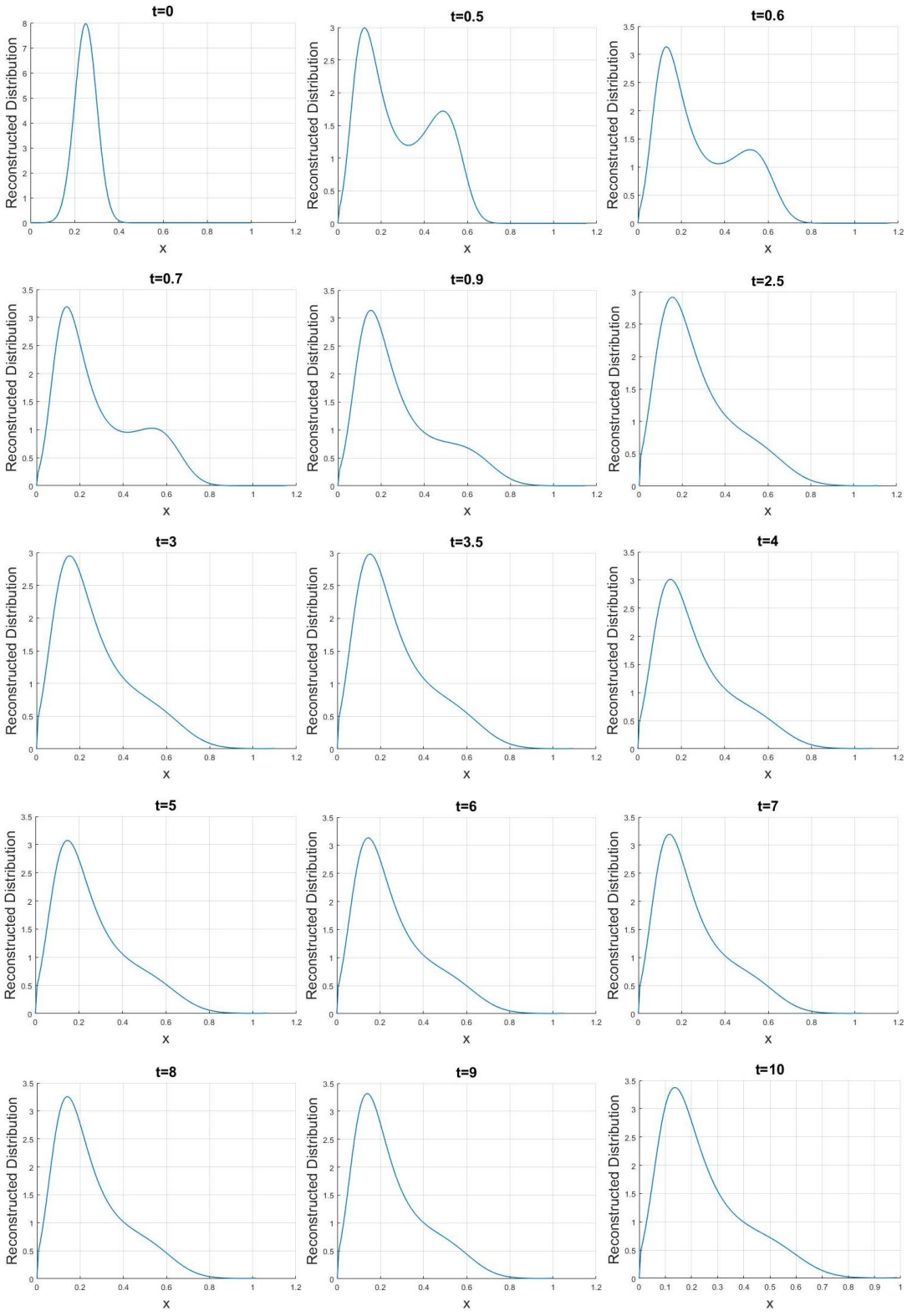

Figure 4.2. Simulation of a cell population using the maximum entropy method in the physical domain. Parameter values:
f=0.25, p=0.1, m=2.

In Figure 4.2. the evolution of the number density function of cells is depicted again, but it can be seen that it takes longer time for the system to reach a steady state solution.

Figure 4.3. illustrates the time evolution of the average intracellular content $\langle x \rangle$ with respect to time t for the case that one uses four, five and six moments in order to reconstruct the density function. It is observed that for five and six moments the evolution of the average intracellular content using the maximum entropy method is almost identical to the one using the finite elements method.

In Figure 4.4. the reconstructed distribution using the maximum entropy method of moments with four, five and six moments is presented and the maximum entropy method is compared with the one computed with the finite elements method. Although the maximum entropy method solves a system of maximum six ordinary differential equations – compared to the one thousand equations that the finite elements method needs to solve - it is shown again that the maximum entropy method presents almost identical results with those of the finite elements method for moments bigger than four as shown below.

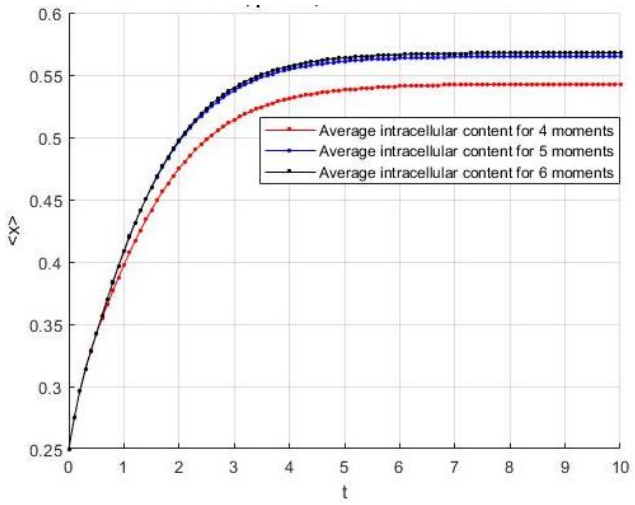

Figure 4.3. Time evolution of average intracellular content with four, five and six moments for f=0.40, p=0.05, m=3,

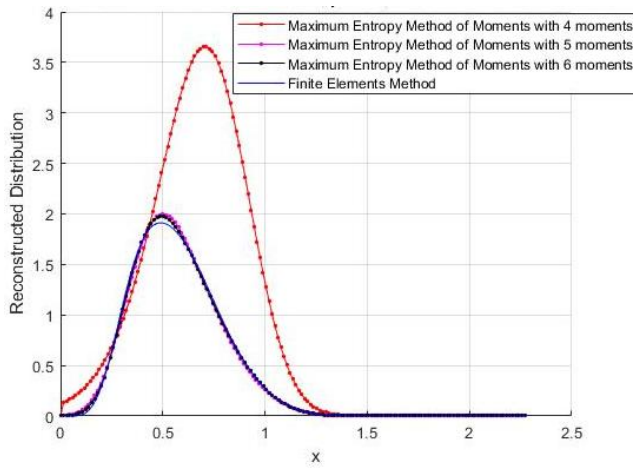

Figure 4.4. Reconstructed distribution for time t=10, with four, five and six moments, for f=0.40, p=0.05, m=3.

In Figures 4.5. and 4.6., the solution of the CPB problem is depicted for the parameter values: $f=0.4, m=1$, $p=0.05$, $\pi=0.03$, $\delta=0.05$, $z_{\max}=4$. The results are presented for time $t=10$ which is the final time of our time integration. Based on the results from the previous example, a number of six moments has been chosen in order to calculate the evolution of the intracellular content with respect to time and the reconstructed density function. In Figure 4.4 the maximum entropy method of moments when applied in the physical domain $\left[0,4\langle x\rangle\right]$ is compared to the normalized domain $[0,1]$. As it is observed, system reaches steady state both in the physical domain and the normalized domain.

Figure 4.6. shows the comparison of the reconstruction of the density function between the maximum entropy method of moments in the physical x and the normalized domain ξ and the finite elements method. It is observed that the results of both the physical and the normalized domain converge to those of the finite elements method again.

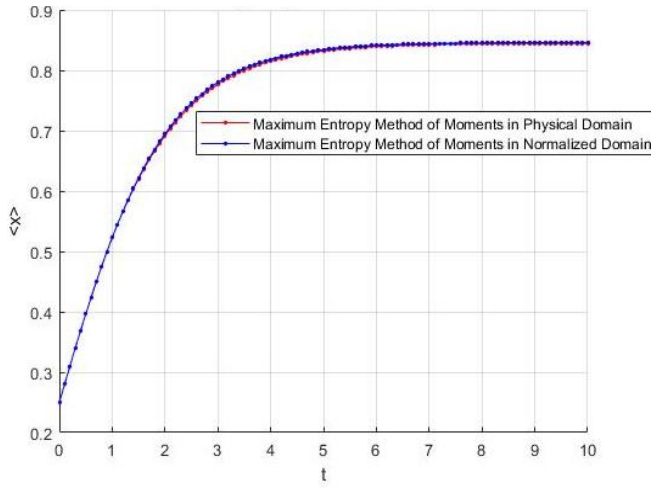

Figure 4.5. Time evolution of average intracellular content with six moments, for f=0.40, p=0.05, m=1.

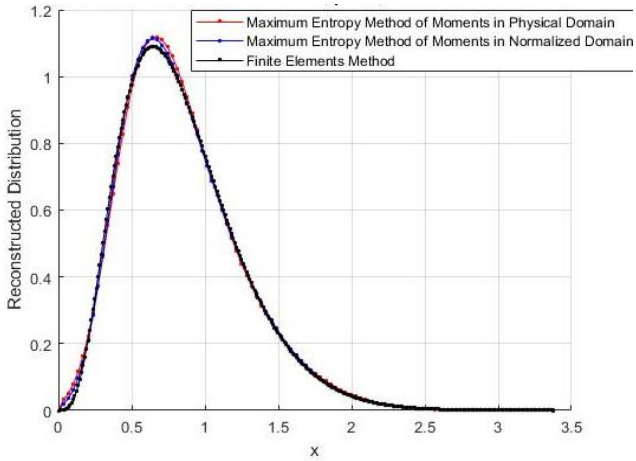

Figure 4.6. Reconstructed distribution for time t=10, with six moments, for f=0.40, p=0.05, m=1.

In Figures 4.7. and 4.8., the solution of the CPB problem is depicted for the following set of parameter values: $f=0.25, m=2$, $p=0.1$, $\pi=0.03$, $\delta=0.05$, $z_{\max}=4$. The results are presented for time $t=10$.

More precisely, Figure 4.7.**,** presents the evolution of the average intracellular content for the physical domain $\left[0,4\langle x\rangle\right]$ and makes the comparison with the one of the normalized domain $[0,1]$. As it is seen, both solutions are quite similar.

Figure 4.8.**,** illustrates the reconstructed distribution as it is calculated using not only the maximum entropy method of moments applied both on the physical and the normalized domain but also the finite elements method using COMSOL multiphysics. It is observed that all the three solutions converge to similar results.

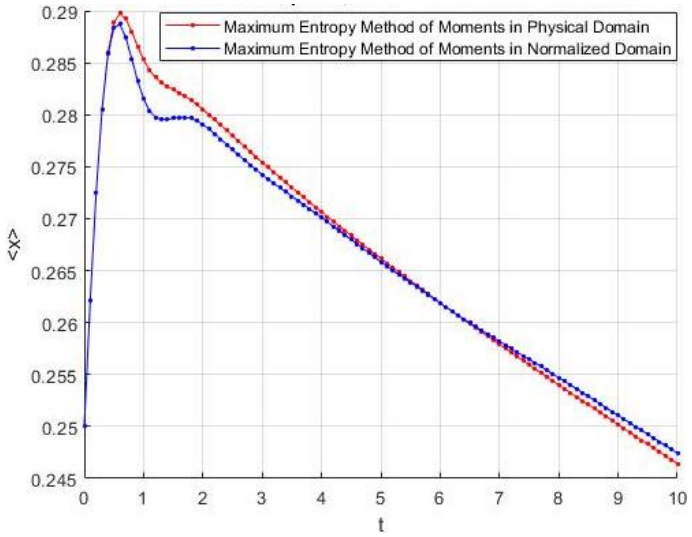

Figure 4.7. Time evolution of average intracellular content with six moments, for f=0.25, p=0.1, m=2.

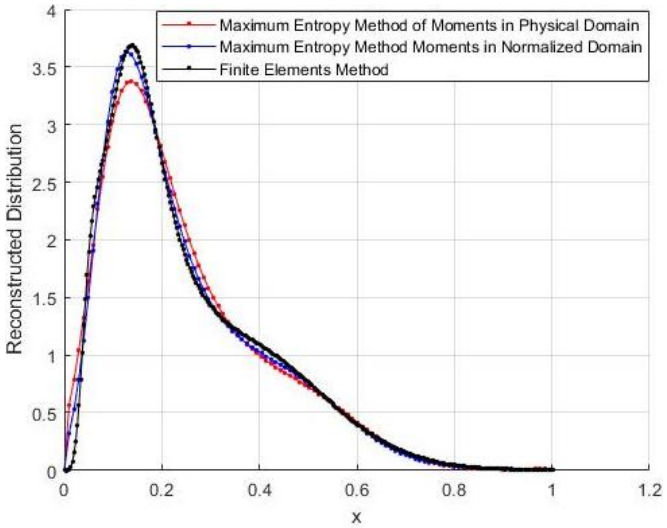

Figure 4.8. Reconstructed distribution for time t=10, with six moments, for f=0.25, p=0.1, m=2**.**

Figures 4.9. and 4.10. depict the solution of the CPB problem for the following set of parameter values: $f = 0.25, m = 2,\ p = 0.05,\ \pi = 0.03,\ \delta = 0.05,\ z_{\max} = 4$. The results of the maximum entropy method of moments both in the physical domain and the normalized domain are compared with those of the finite elements method using COMSOL Multiphysics.

More precisely, Figure 4.9.**,** presents the evolution of the average intracellular content for the physical domain $\left[0, 4\langle x\rangle\right]$ and makes the comparison with the one of the normalized domain $[0,1]$. As it is seen both solutions are identical.

In Figure 4.10., the reconstructed distribution of the density function is presented. The results of the maximum entropy method of moments are compared with those of the finite elements method and as it can be seen they are almost identical. A small error between the solution of the maximum entropy method and the finite elements is presented, but it is quite small if one thinks that maximum entropy method of moments solves 6 ODEs while finite elements solve one thousand of them.

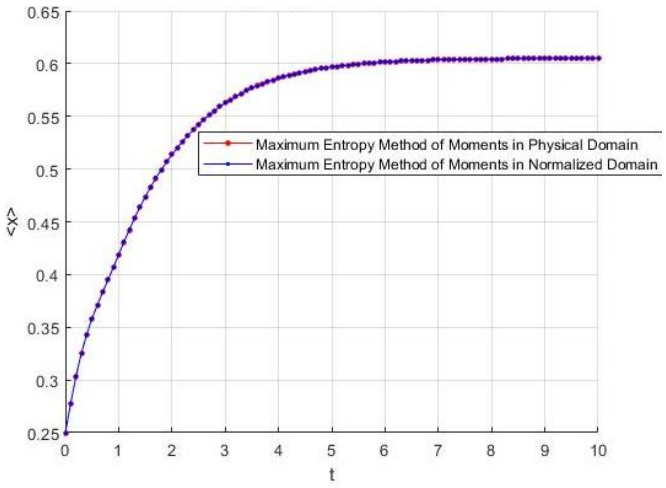

Figure 4.9. Time evolution of average intracellular content with seven moments, for f=0.25, p=0.05, m=2.

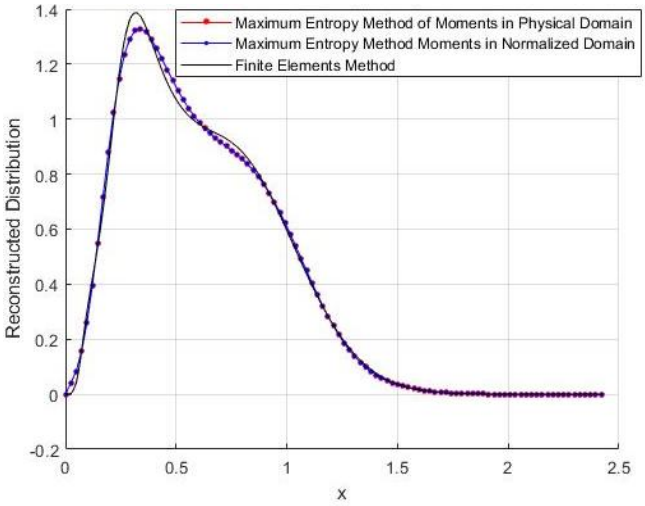

Figure 4.10. Reconstructed distribution for time t=10, with seven moments, for f=0.25, p=0.05, m=2.

In Figures 4.11. and 4.12., the solution of the CPB problem is depicted for the following set of parameter values: $f = 0.25, m = 2$, $p = 0.15$, $\pi = 0.03$, $\delta = 0.05$, $z_{\max} = 4$. The results are presented for time $t = 10$ at which the system has reached a steady state solution.

Figure 4.11. illustrates the evolution of the average intracellular content for the chosen time interval [0,10]. As it is easily observed system reaches steady state in physical domain and the comparison is made between physical domain and COMSOL Multiphysics. Figure 4.12., shows the reconstructed distribution of the density function for the physical domain $\left[0, 4\langle x \rangle\right]$ and it is shown that the solution of maximum entropy method of moments is quite similar with the one of the finite elements method.

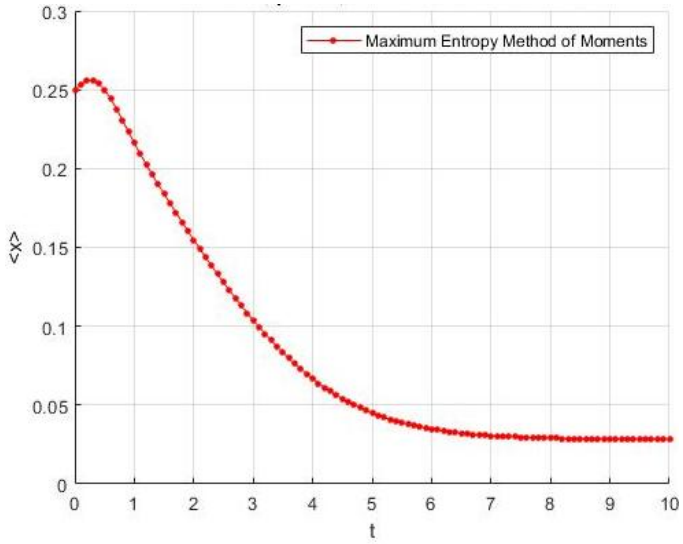

Figure 4.11. Time evolution of average intracellular content with seven moments, for f=0.25, p=0.15, m=2.

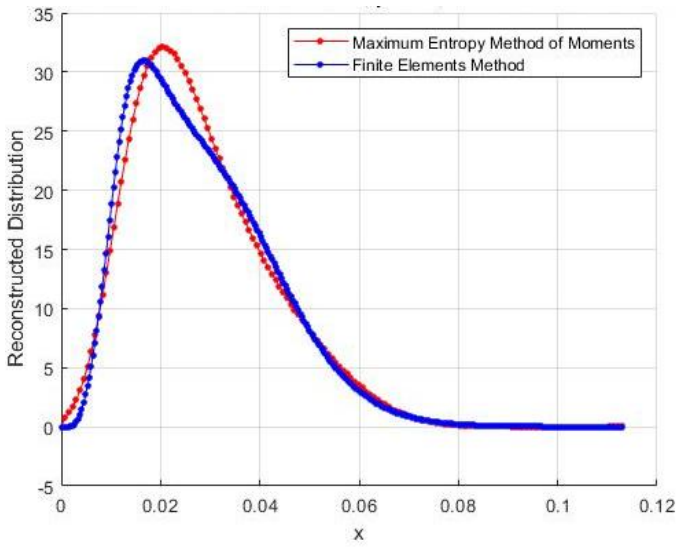

Figure 4.12. Reconstructed distribution for time t=10, with seven moments, for f=0.25, p=0.15, m=2.

Figures 4.13. and 4.14. depict the solution of the CPB problem for the following set of parameter values: $f = 0.40, m = 2,\ p = 0.15,\ \pi = 0.03,\ \delta = 0.05,\ z_{\max} = 4$. The results are presented for time $t = 10$, however it seems that this time the system has not reached a steady state solution yet.

More precisely, Figure 4.13.**,** presents the evolution of the average intracellular content for the physical domain $\left[0, 4\langle x \rangle\right]$ and makes the comparison with the one of the normalized domain $[0,1]$. As it is seen both solutions are totally identical.

In Figure 4.14., the reconstructed distribution of the density function is presented. The results of the maximum entropy method of moments are compared with those of the finite elements method and as it can be seen they are quite similar. It seems that in this case the maximum entropy method of moments in the normalized domain works better than this in the physical domain. However, all the three solutions are close enough.

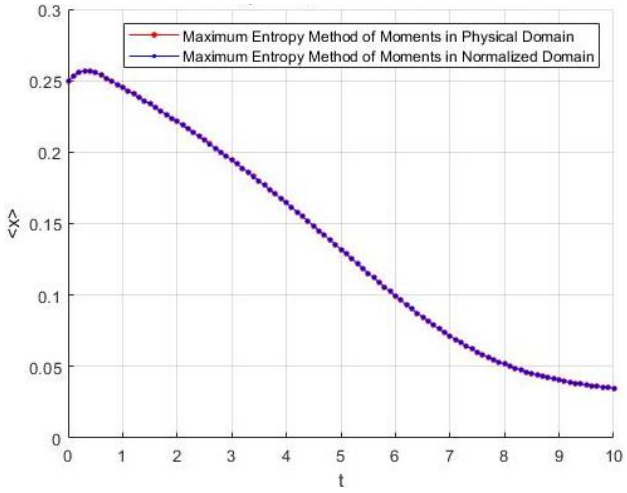

Figure 4.13. Time evolution of average intracellular content with seven moments for f=0.40, p=0.15, m=2.

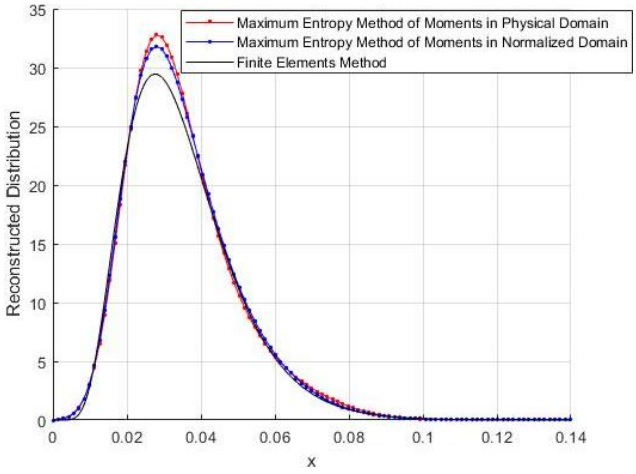

Figure 4.14. Reconstructed distribution for time t=10, with seven moments for f=0.40, p=0.15, m=2.

4.3.2 Symmetric partitioning

Symmetric partitioning is another way to express the CPB problem of the isogenic cell population with Lac Operon genetic network and rewrite the formulas in order to use maximum entropy method moments and conclude to a solution. As it was seen in (4.16) the partition probability density function changes and the mother cells stop giving their intracellular content under discrete values to the daughter cells and start sharing their intracellular content under a specific probability. As a consequence, the results that have to do with the alteration of the allocation of the cells, the average intracellular content evolution and the reconstruction of the density function change dramatically. Next, we present simulations performed with maximum entropy method of moments for various parameter values of L and p and compare the results against a finite element code which was implemented in **(Kavousanakis et al. 2009)** using COMSOL Multiphysics.

The results of a transient simulation of the system of equations of isogenic cell population with Lac Operon genetic network is depicted in Figure 4.15. for the following parameter values: $L = 5,\ q = 2,\ p = 0.15,\ \pi = 0.03$ and $\delta = 0.5$.

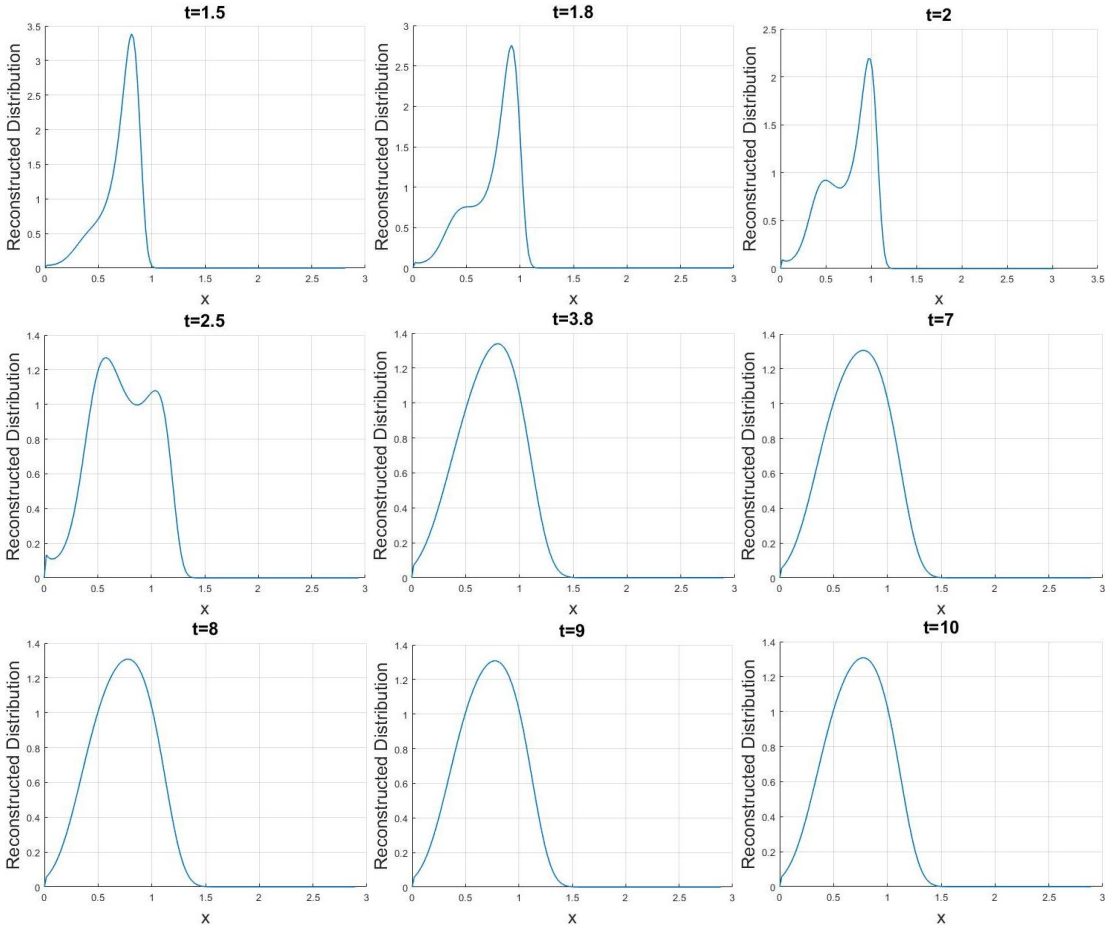

Figure 4.15. Simulation of a cell population using the maximum entropy method for the symmetric partitioning case. Parameter values:
L=5, q=2, p=0.15, π=0.03, δ=0.5 and six moments.

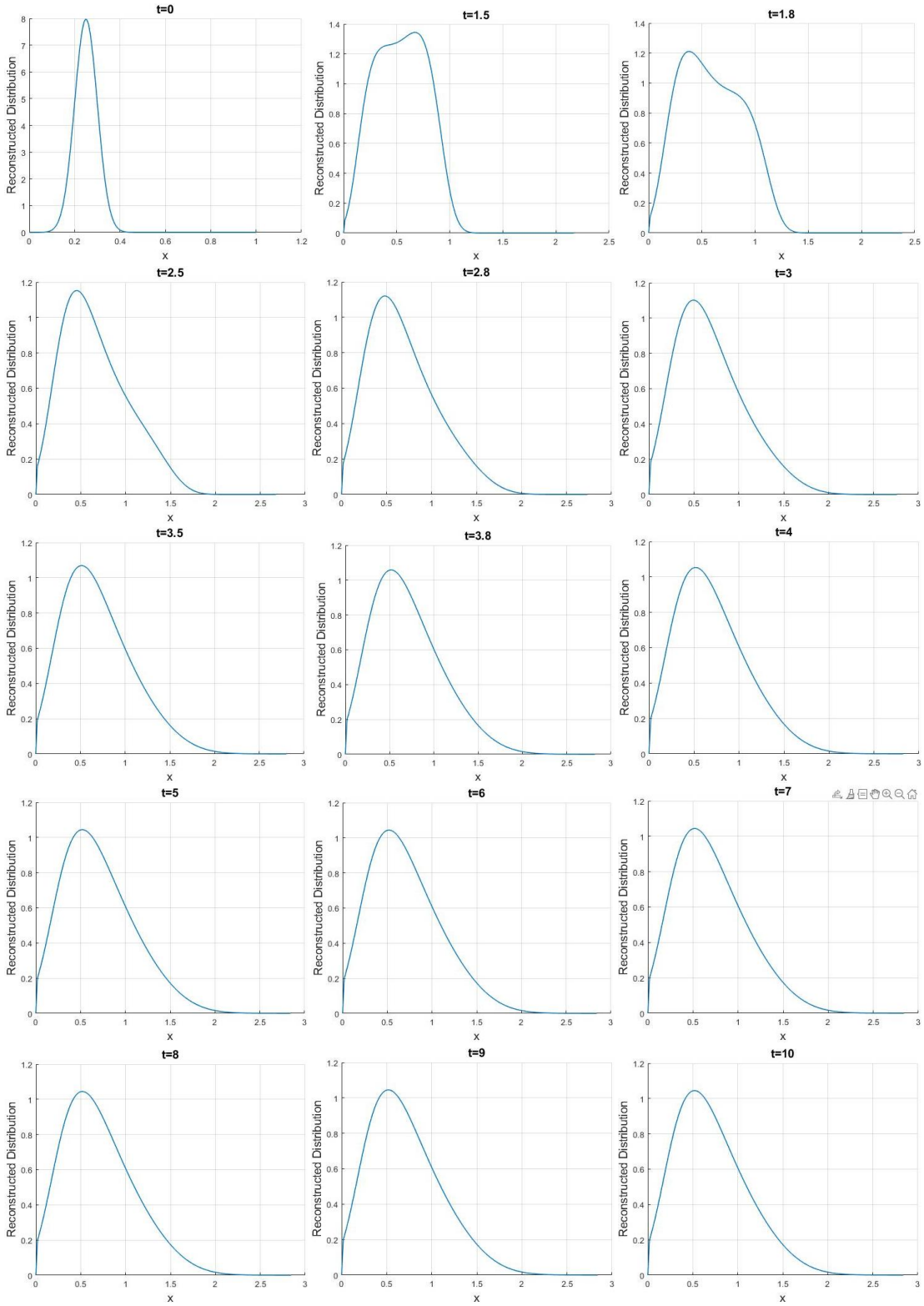

Figure 4.16. Simulation of a cell population using the maximum entropy method for the symmetric partitioning case. Parameter values:
L=2, q=2, p=0.4, π=0.03, δ=0.05 and seven moments.

Figure 4.16. illustrates the evolution of the number density function of cells. It is observed that cell density function fluctuates from t=1.5 to t=3 and after that time our system converges to a steady state solution.

Figures 4.17. and 4.18. depict the solution of the CPB problem for parameter values: $L=5, q=2$, $p=0.15$, $\pi=0.03$, $\delta=0.5$. The results are presented for time $t=1$ and the moments on the specific time are chosen for the reconstruction, in order to check that the whole system has converged and has reached the desirable steady state situation.

More precisely, Figure 4.17., illustrates the evolution of the average intracellular content for the chosen time domain [0,10]. As it is easily observed system reaches steady state and there is almost total concurrence between Maximum Entropy and Comsol Multiphysics results. Figure 4.18. shows the reconstructed distribution evolution from 0 to $4\langle x\rangle$.

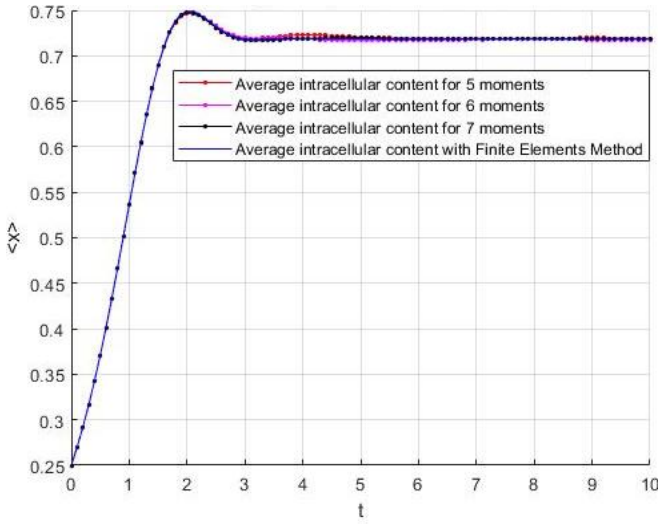

Figure 4.17. Time evolution of average intracellular content
with five, six and seven moments, for L=5, q=2, p=0.15, π=0.03, δ=0.5.

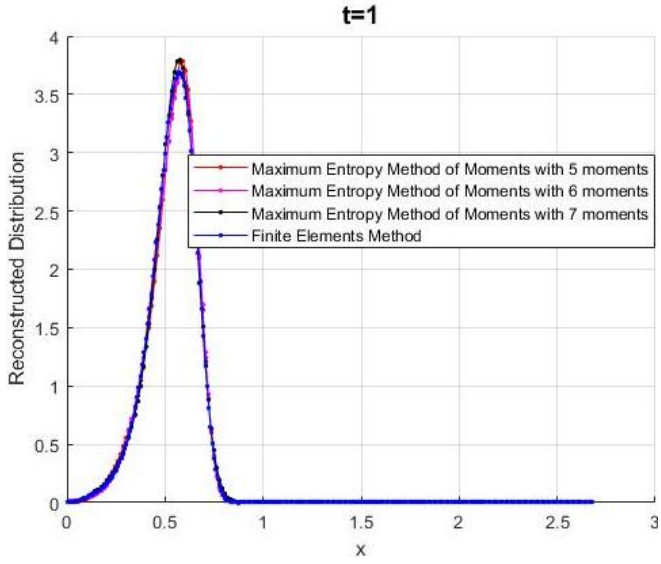

Figure 4.18. Reconstructed distribution
with five, six and seven moments for L=5, q=2, p=0.15, π=0.03, δ=0.5

Figures 4.19., 4.20. and 4.21. depict the reconstructed density function of the CPB problem for the parameter values: $L=5, q=2$, $p=0.15$, $\pi=0.03$, $\delta=0.5$. The results are presented for times $t=2$, $t=2.5$ and $t=10$. For all time instances, the maximum entropy method of moments with the seven moments appears increasing accuracy in comparison with the five moments and the four moments, because its results are almost identical with those of the finite elements method.

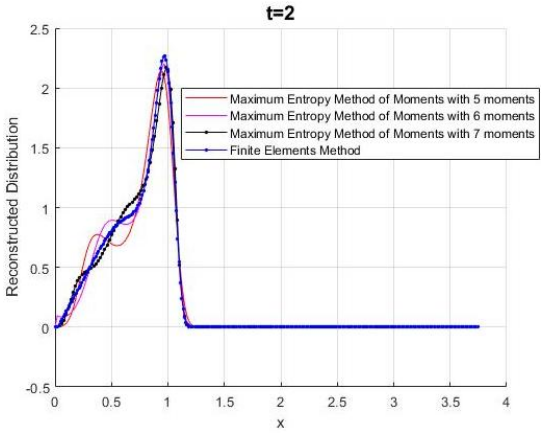

Figure 4.19. Reconstructed distribution
with five, six and seven moments, for L=5, q=2, p=0.15.

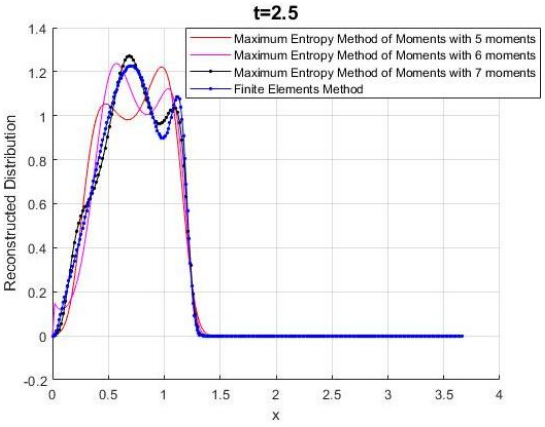

Figure 4.20. Reconstructed distribution
with five, six and seven moments, for L=5, q=2, p=0.15.

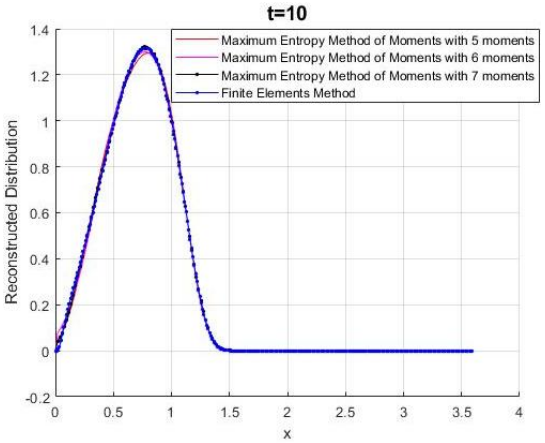

Figure 4.21. Reconstructed distribution
with five, six and seven moments, for L=5, q=2, p=0.15.

Figure 4.22. depicts the evolution of the average intracellular content for the chosen time domain [0,10]. After a specific period, the system reaches steady state and there is almost total concurrence between the maximum entropy method of moments and the COMSOL Multiphysics results.

In Figure 4.23., the reconstructed density function is presented and it can be seen that the calculated with maximum entropy method of moments density function coincides totally with the one calculated with the finite elements method. The results are presented for time $t = 0.5$ and the chosen parameters for our model are $L = 2$, $q = 2$, $p = 0.4$, $\pi = 0.03$, $\delta = 0.05$.

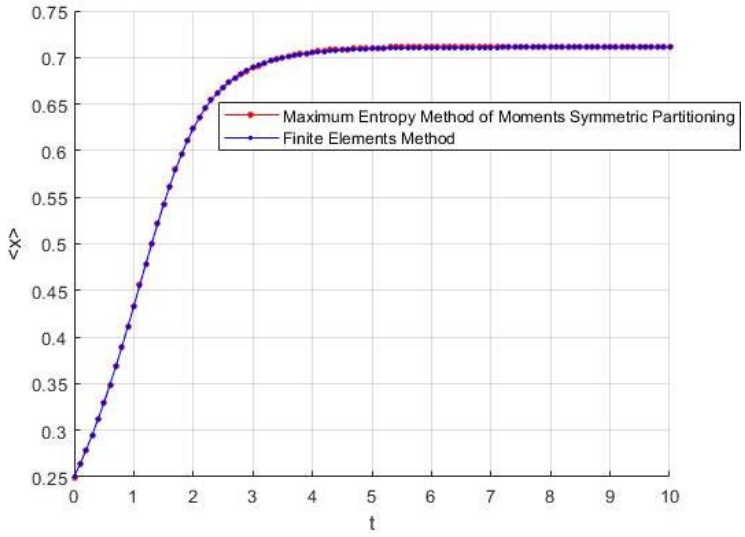

Figure 4.22. Time evolution of average intracellular content with seven moments, for L=2, q=2, p=0.4, π=0.03, δ=0.05.

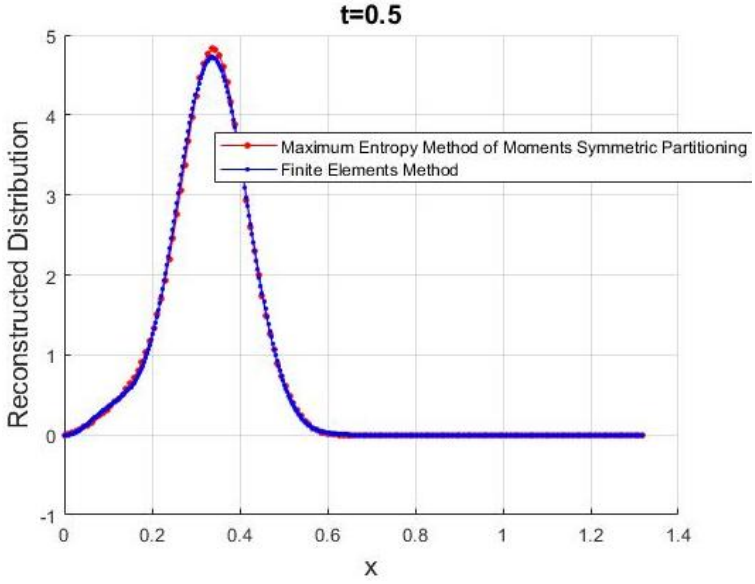

Figure 4.23. Reconstructed distribution with seven moments, for L=2, q=2, p=0.4, π=0.03, δ=0.05.

Figures 4.24., 4.25. and 4.26. depict the solution of the CPB problem for parameter values: $L=2, q=2,\ p=0.4,\ \pi=0.03,\ \delta=0.05$. The results are presented for times $t=1,\ t=2$ and $t=10$. For all three cases, the power that the maximum entropy method of moments has is demonstrated. Even for t=2 the maximum entropy method of moments reaches a very satisfying approximation of the real solution, proving once again its power compared to the finite elements method.

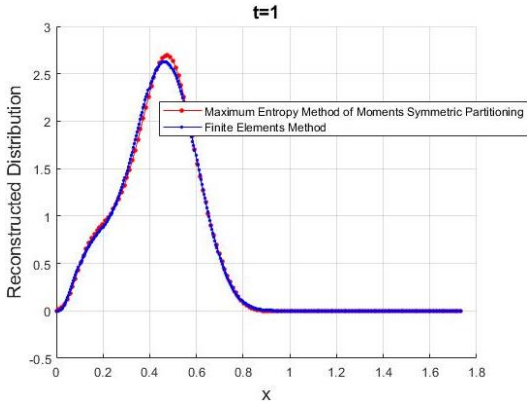

Figure 4.24. Reconstructed distribution with seven moments, for L=2, q=2, p=0.4, π=0.03, δ=0.05.

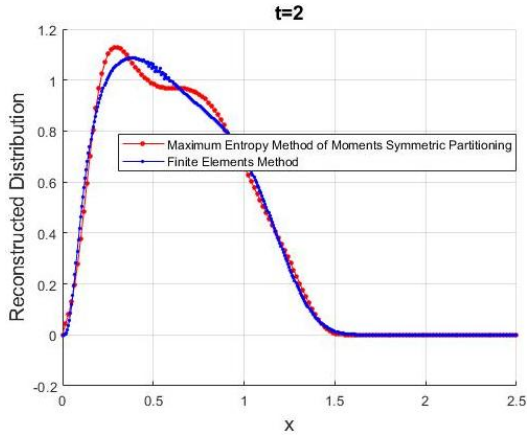

Figure 4.25. Reconstructed distribution with seven moments, for L=2, q=2, p=0.4, π=0.03, δ=0.05.

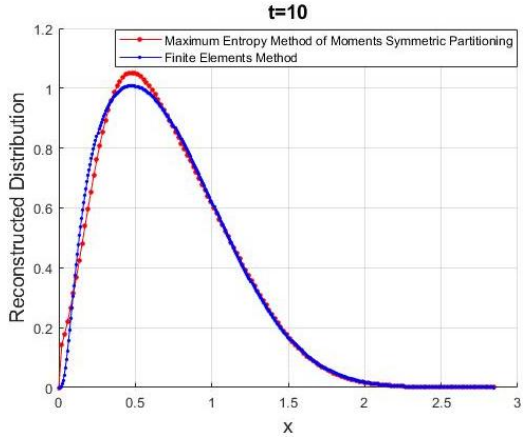

Figure 4.26. Reconstructed distribution with seven moments, for L=2, q=2, p=0.4, π=0.03, δ=0.05.

Figure 4.27., illustrates the evolution of the average intracellular content for the chosen time domain [0,20]. It is observed that there is total convergence between the maximum entropy method of moments and the finite elements method results. It must be pointed that even though the maximum entropy method of moments solved a system of only seven integral differential equations, it appeared total concurrence with the finite elements method that solved a system of one thousand equations.

In Figure 4.28.**,** it can be seen that the reconstructed density function using the maximum entropy method of moments has converged totally with the one calculated with the finite elements method. The results are presented for time $t = 0.5$ and the chosen parameters of our model are $L = 2, q = 2,\ p = 0.4,\ \pi = 0.03,\ \delta = 0.05$.

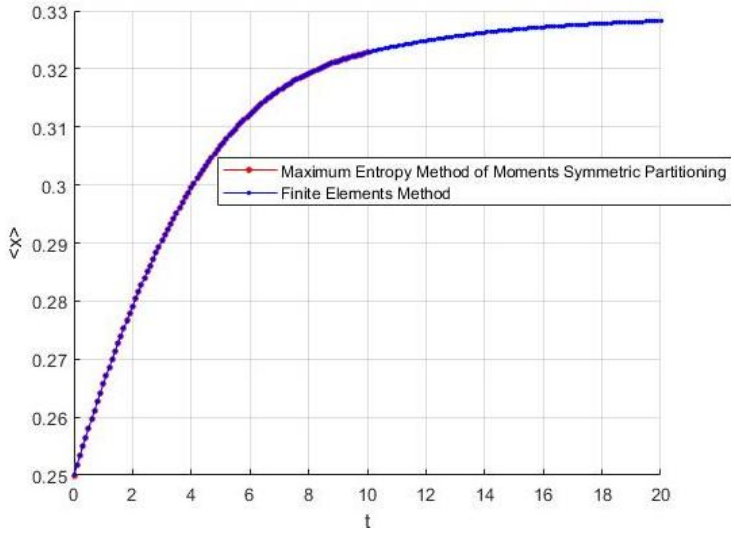

Figure 4.27. Time evolution of average intracellular content with seven moments, for L=2, q=2, p=4, π=0.03, δ=0.05.

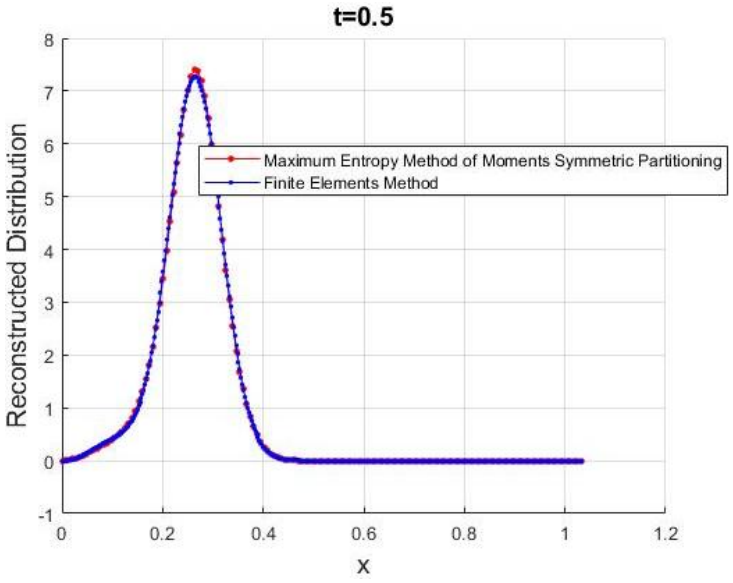

Figure 4.28. Reconstructed distribution with seven moments, for L=2, q=2, p=4, π=0.03, δ=0.05.

Figures 4.29., 4.30. and 4.31. depict the solution of the CPB problem for parameter values: $L=2, q=2,\ p=0.4,\ \pi=0.03,\ \delta=0.05$. The results are presented for times $t=1,\ t=5$ and $t=10$.

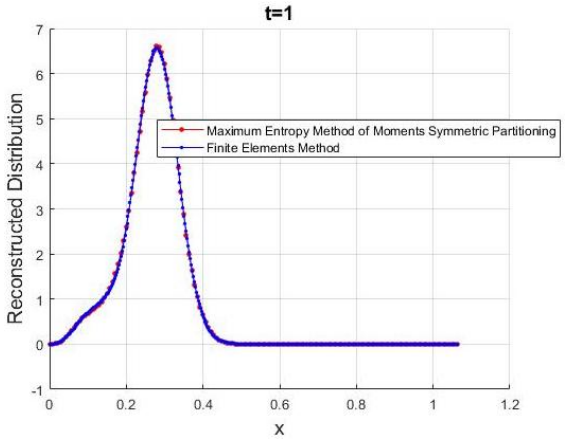

Figure 4.29. Reconstructed distribution with seven moments, for L=2, q=2, p=4, π=0.03, δ=0.05.

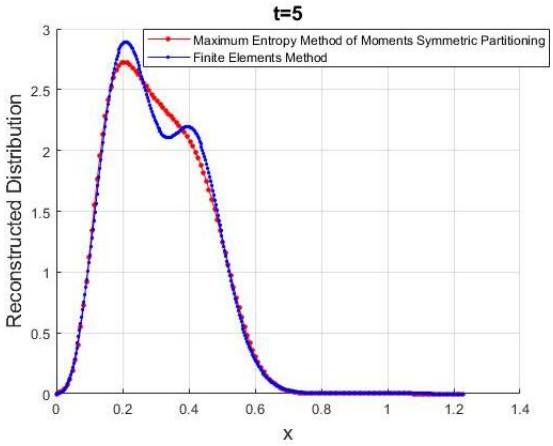

Figure 4.30. Reconstructed distribution with seven moments, for L=2, q=2, p=4, π=0.03, δ=0.05.

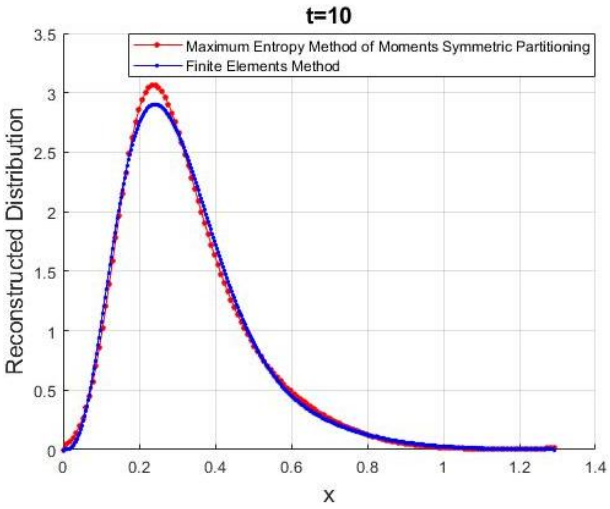

Figure 4.31. Reconstructed distribution with seven moments, for L=2, q=2, p=4, π=0.03, δ=0.05.

Figure 4.32. illustrates the evolution of the average intracellular content for the chosen time domain [0,20]. As it is observed system reaches the steady state situation and there is almost total concurrence between maximum entropy method of moments and the COMSOL Multiphysics results.

Figure 4.33. presents the reconstructed distribution of the density function for the domain $\left[0,4\langle x\rangle\right]$. The results are presented for time $t=0.5$ and the chosen parameters of the CPB model are $L=5, q=2,\ p=4,\ \pi=0.03,\ \delta=0.5$.

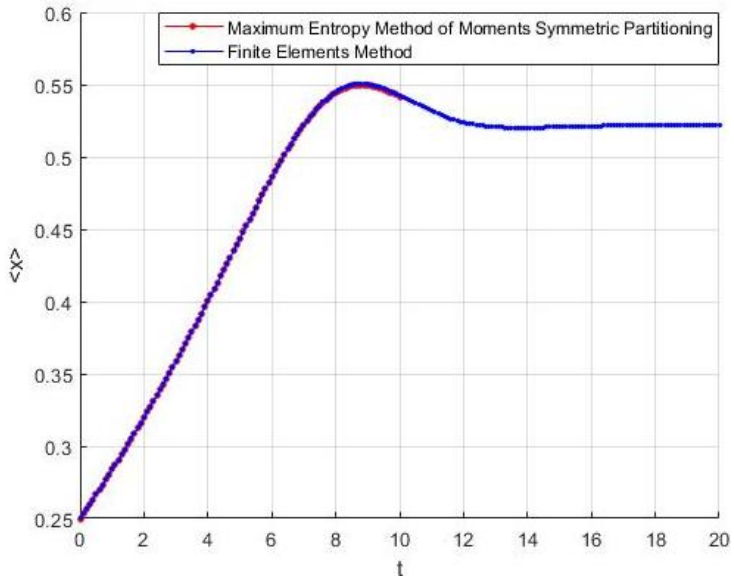

Figure 4.32. Time evolution of average intracellular content with seven moments for L=5, q=2, p=4, π=0.03, δ=0.05.

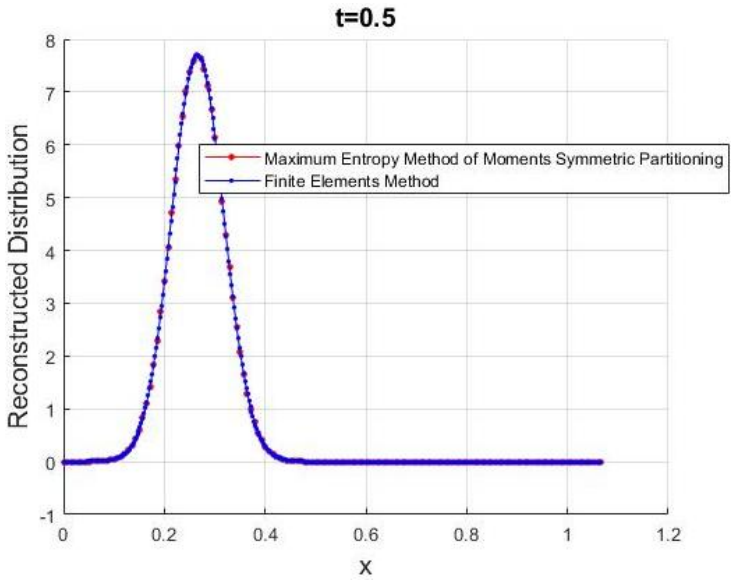

Figure 4.33. Reconstructed distribution with seven moments, for L=5, q=2, p=4, π=0.03, δ=0.05.

Figures 4.34., 4.35. and 4.36. depict the solution of the CPB problem for parameter values: $L=5, q=2,\ p=4,\ \pi=0.03,\ \delta=0.5$. The results are presented for times $t=5,\ t=10$ and $t=20$.

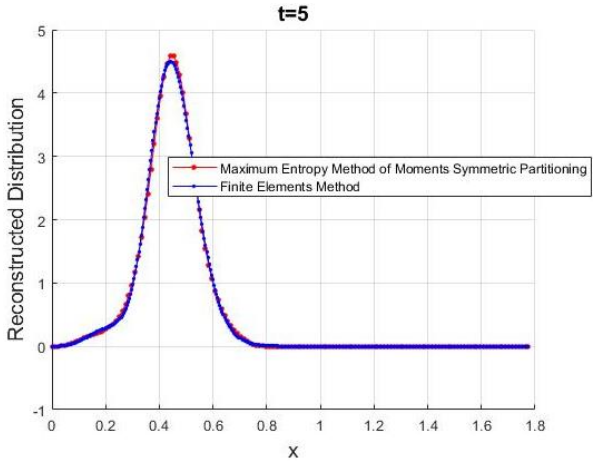

Figure 4.34. Reconstructed distribution with seven moments, for L=5, q=2, p=4, π=0.03, δ=0.05.

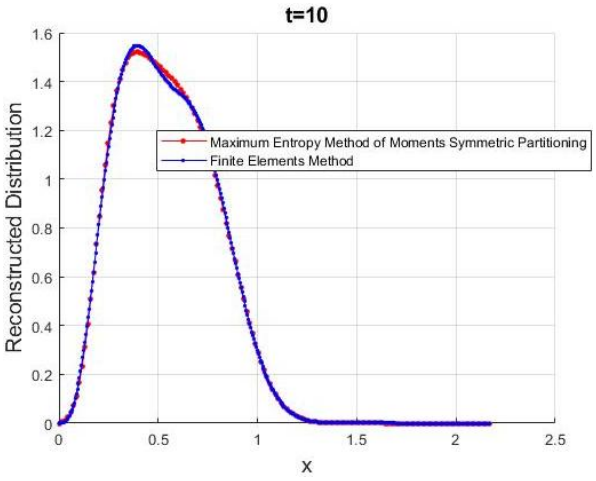

Figure 4.35. Reconstructed distribution with seven moments, for L=5, q=2, p=4, π=0.03, δ=0.05.

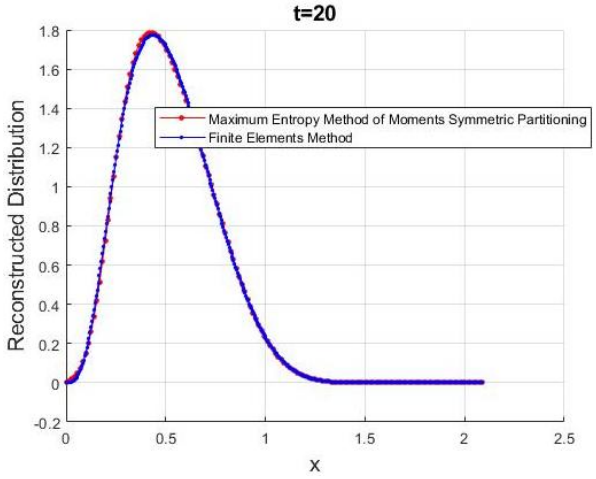

Figure 4.36. Reconstructed distribution with seven moments, for L=5, q=2, p=4, π=0.03, δ=0.05.

5 Conclusion and future work

The basic goal of this diploma thesis is the development of a computational framework, which transforms partial-integro-differential equations –which are used for the E Coli isogenic populations with the Lac Operon genetic network- into a set of ordinary differential equations modeling the evolution of moments of the distribution of cells with respect to their intracellular content.

Under the greater spectrum of those assumptions the dynamic behavior of this kind of populations has been studied and the results of the maximum entropy method of moments algorithm are compared against a finite elements code which was implemented by **(Kavousanakis et al. 2009)** with the COMSOL Multiphysics.

First, we presented the application of the maximum entropy algorithm in order to reconstruct known distribution functions given a small number of low order moments. Based on the algorithm, we calculated the Lagrangian multipliers and then reconstructed the distribution. In particular, we demonstrated its very good performance by reconstructing unimodal and bimodal distributions.

Then, we derived from the CPB model the moment evolution equations. A closure expression for the number density function is derived using the maximum entropy method of moments. Then, we performed simulations of the maximum entropy method of moments algorithm for different parameter values. In all cases, the proposed method was able to capture the abrupt dynamics of the distribution function which were observed at the initial stages of the simulation, and it still captured the long time dynamics which converged to steady state solutions. The comparison against a finite elements code shows that the maximum entropy method of moments can compute successfully the moments for the distribution, as well as can capture adequately well the shape of the density function. Regarding the convenience of capturing the shape of the density function, a big enough number of moments has to be used. A number of six or seven moments can be used and have satisfactory accuracy even capturing the shape of number density functions as computed from the finite elements method. This approximation reduces significantly the computational cost, since we only have to solve a system of six or seven ordinary differential equations instead of dealing with systems of approximately one thousand degrees of freedom (resulting in from the finite elements discretization of the partial-integro-differential equations). The cases which have been solved in this diploma thesis deal with symmetric and asymmetric partitioning of a cell population; in both cases, we demonstrated the ability of maximum entropy method of moments to reach adequately well the solution even when solving a small system of ordinary differential equations.

An extension of this work could be for CPBs in two or higher dimensions. The computational requirements of the finite elements solution of such systems are largely enhanced, thus the maximum entropy method of moments (with significantly lower requirements) can be a promising alternative for capturing the evolution of the density statistics, as well as capturing adequately well the shape of distribution functions of

cell populations. It would also be interesting to explore the possibility of performing parametric continuation and stability analysis using. In particular for the lac operon genetic network that features bistability, it would be interesting to study the possibility of implementing steady-state algorithms (Newton-Raphson), parametric continuation algorithms (pseudo arc-length continuation), and eigenvalue solvers wrapped around the maximum entropy method of moments. Such an analysis can bypass the need to perform dynamic evolution simulations for an extensively large set of parameter values and enable to compute the total solution space using only a few equations for the moments of cell distribution functions.

References

Abboud AW, Schroeder BB, Saad T, et al (2015) A numerical comparison of precipitating turbulent flows between large-eddy simulation and one-dimensional turbulence. AIChE J 61:3185–3197. https://doi.org/10.1002/aic.14870

Aviziotis IG, Kavousanakis ME, Bitsanis IA, Boudouvis AG (2015) Coarse-grained analysis of stochastically simulated cell populations with a positive feedback genetic network architecture. J Math Biol 70:1457–1484. https://doi.org/10.1007/s00285-014-0799-2

Diemer RB, Olson JH (2002) A moment methodology for coagulation and breakage problems: Part 3-generalized daughter distribution functions. Chem Eng Sci 57:4187–4198. https://doi.org/10.1016/S0009-2509(02)00366-4

Elowitz MB, Levine AJ, Siggia ED, Swain PS (2002) Stochastic gene expression in a single cell. Science (80-) 297:1183–1186. https://doi.org/10.1126/science.1070919

Falola A, Borissova A, Wang XZ (2013) Extended method of moment for general population balance models including size dependent growth rate, aggregation and breakage kernels. Comput Chem Eng 56:1–11. https://doi.org/10.1016/j.compchemeng.2013.04.017

Frenklach M (2002) Method of moments with interpolative closure. Chem Eng Sci 57:2229–2239. https://doi.org/10.1016/S0009-2509(02)00113-6

Hounslow MJ, Ryall RL, Marshall VR (1988) A discretized population balance for nucleation, growth, and aggregation. AIChE J 34:1821–1832. https://doi.org/10.1002/aic.690341108

Kavousanakis ME, Mantzaris N V., Boudouvis AG (2009) A novel free boundary algorithm for the solution of cell population balance models. Chem Eng Sci 64:4247–4261. https://doi.org/10.1016/j.ces.2009.06.054

Kepler TB, Elston TC (2001) Stochasticity in transcriptional regulation: Origins, consequences, and mathematical representations. Biophys J 81:3116–3136. https://doi.org/10.1016/S0006-3495(01)75949-8

Lee KW (1983) Change of particle size distribution during Brownian coagulation. J Colloid Interface Sci 92:315–325. https://doi.org/10.1016/0021-9797(83)90153-4

Lin Y, Lee K, Matsoukas T (2002) Solution of the population balance equation using constant-number Monte Carlo. Chem Eng Sci 57:2241–2252. https://doi.org/10.1016/S0009-2509(02)00114-8

Mantzaris N V. (2006) Stochastic and deterministic simulations of heterogeneous cell population dynamics. J Theor Biol 241:690–706. https://doi.org/10.1016/j.jtbi.2006.01.005

Mantzaris N V. (2007) From single-cell genetic architecture to cell population dynamics: Quantitatively decomposing the effects of different population heterogeneity sources for a genetic network with positive feedback architecture. Biophys J 92:4271–4288. https://doi.org/10.1529/biophysj.106.100271

Mantzaris N V. (2005) A cell population balance model describing positive feedback loop expression dynamics. Comput Chem Eng 29:897–909. https://doi.org/10.1016/j.compchemeng.2004.09.012

Mantzaris N V., Daoutidis P, Srienc F (2001) Numerical solution of multi-variable cell population balance models. II. Spectral methods. Comput Chem Eng 25:1441–1462. https://doi.org/10.1016/S0098-1354(01)00710-4

McGraw R (1997) Description of aerosol dynamics by the quadrature method of

moments. Aerosol Sci Technol 27:255–265. https://doi.org/10.1080/02786829708965471

Mead LR, Papanicolaou N (1984) Maximum entropy in the problem of moments. J Math Phys 25:2404–2417. https://doi.org/10.1063/1.526446

Ramkrishna D (2008) Population Balances

Randolph AD, Larson MA (1971) Analysis and Techniques of Continuous Crystallisation New York and London

Saad T, Ruai G (2019) PyMaxEnt: A Python software for maximum entropy moment reconstruction. SoftwareX 10:100353. https://doi.org/10.1016/j.softx.2019.100353

Subramanian G, Ramkrishna D (1971) On the solution of statistical models of cell populations. Math Biosci 10:1–23. https://doi.org/10.1016/0025-5564(71)90050-2

Zhu GY, Zamamiri A, Henson MA, Hjortsø MA (2000) Model predictive control of continuous yeast bioreactors using cell population balance models. Chem Eng Sci 55:6155–6167. https://doi.org/10.1016/S0009-2509(00)00208-6